Public Disclosure Authorized

Public Disclosure Authorized

Policy Research Working Paper 11451

Housing Requirements, Hazard Exposure, and Resilience Costs

A Global Outlook to 2100

Yasuhiro Kawasoe



WORLD BANK GROUP
Urban, Disaster Risk Management,
Resilience and Land Global Department
September 2026



Reproducible Research Repository

A verified reproducibility package for this paper is available at http://reproducibility.worldbank.org, click **here** for direct access.

Policy Research Working Paper 11451

Abstract

Global housing demand is rising rapidly, yet the combined pressures of future population growth, climate-driven hazard intensification, and constrained fiscal capacity have not been assessed together for their impact on housing at a global scale. Housing is one of the largest components of household wealth and national capital stock. This study provides the first global, country-level picture of future housing construction demand and its associated costs and identifies where the needs for resilient construction are most urgent. The lack of high-resolution, globally consistent geospatial and demographic data has limited previous analyses. This study integrates Shared Socioeconomic Pathways–based population projections to 2100 with dynamic household size modeling, cohort survival analysis, and multi-hazard exposure mapping to estimate future housing construction demand and its associated costs under business-as-usual and resilient construction pathways. Global housing stock is projected to nearly double by 2100, reaching 4.1 billion to 4.5 billion units. Resilient construction pathways are found to carry lower long-term costs than business-as-usual in most regions, although not in high-growth, high-hazard regions such as South Asia and Sub-Saharan Africa. Construction demand in most regions is projected to transition from growth-driven to replacement-driven by mid-century, suggesting that the decisions made today about how and where it is built will shape countries' exposure to natural hazards and their fiscal obligations for decades to come. The study further identifies 46 countries facing a triple burden: high future housing demand, severe natural hazard exposure, and limited fiscal capacity to finance resilient construction. The nature of this burden varies systematically by region, with Pacific Island countries facing acute fiscal constraints, Sub-Saharan Africa facing unprecedented volumetric demand, and South and Southeast Asian countries facing the highest hazard exposure. These findings provide a quantitative basis for prioritizing resilient housing investment, nationally and through international support, differentiated across regions and individual countries.

This paper is a product of the Urban, Disaster Risk Management, Resilience and Land Global Department. It is part of a larger effort by the World Bank to provide open access to its research and make a contribution to development policy discussions around the world. Policy Research Working Papers are also posted on the Web at http://www.worldbank.org/prwp. The author may be contacted at ykawasoe@worldbankgroup.org. A verified reproducibility package for this paper is available at http://reproducibility.worldbank.org, click **here** for direct access.



The Policy Research Working Paper Series disseminates the findings of work in progress to encourage the exchange of ideas about development issues. An objective of the series is to get the findings out quickly, even if the presentations are less than fully polished. The papers carry the names of the authors and should be cited accordingly. The findings, interpretations, and conclusions expressed in this paper are entirely those of the authors. They do not necessarily represent the views of the International Bank for Reconstruction and Development/World Bank and its affiliated organizations, or those of the Executive Directors of the World Bank or the governments they represent.

Produced by the Research Support Team

Housing Requirements, Hazard Exposure, and Resilience Costs: A Global Outlook to 2100

Authorized for distribution by Niels B. Holm-Nielsen, Manager, Urban, Disaster Risk Management, Resilience and Land Global Department, World Bank Group

Keywords: Housing demand; resilient construction; climate change; natural hazard exposure; fiscal capacity; population projections.
JEL codes: R31, Q54, H84, I32, J11, O18

1. Introduction

Over the coming decades, the world will construct an enormous volume of new housing, concentrated in regions where natural hazard exposure is high and institutional capacity to regulate and enforce safe construction is limited. Housing is typically the largest asset households own and one of the largest components of the built environment, and its quality shapes health outcomes, poverty dynamics, and the scale of losses when disasters strike. The decisions embedded in that construction, such as where to build, at what quality, and to what hazard-resistance standard, will determine disaster risk and development outcomes for housing, people, and livelihoods for the remainder of this century. Current estimates place the global housing deficit at approximately 268 million units, affecting 1.26 billion people across 64 emerging economies (Behr et al., 2021), and national assessments consistently suggest this figure understates the true scope. Across the globe, housing deficits are large, growing, and structurally embedded in patterns of urbanization, income inequality, and limited institutional capacity.

The housing deficit has two dimensions, and both are relevant to disaster risk. The quantitative deficit refers to the shortage of available dwellings relative to the number of households requiring housing. Nigeria estimates a shortage of 17 million to 30 million units (World Bank, 2016), India projects a shortage of 30 million units by 2030 (Knight Frank & NAREDCO, 2025), and Indonesia requires approximately 780,000 new units annually through 2045 (World Bank, 2020). The qualitative deficit refers to households living in substandard or structurally inadequate housing, such as dwellings with insecure foundations, incomplete walls or roofing, or severe overcrowding, and this dimension is often larger than the quantitative one. In Colombia, 73 percent of the total housing deficit is qualitative in nature (World Bank, 2021); in El Salvador, 72 percent of households experience some form of housing deprivation (World Bank, 2024). These figures are not only welfare indicators but also a measure of structural vulnerability, as the conditions that define the qualitative deficit are the same conditions that determine how housing performs when hazards occur.

Housing demand is not driven by population growth alone, and this distinction matters for understanding where and how fast the deficit will expand. Global population is projected to peak at approximately 10.3 billion people in the mid-2080s (United Nations Department of Economic and Social Affairs, 2024), but a more immediate pressure comes from the structural decline in household size (United Nations Department of Economic and Social Affairs, 2019). The global average household size has declined by approximately 0.5 person per decade since 1970 (Esteve et al., 2024). As incomes rise and family structures evolve, more households form from the same population base, amplifying demand beyond what population projections alone would imply. In developing economies, this additional

demand is unlikely to be absorbed by formal housing markets, which remain inaccessible to low-income households due to high costs, restrictive financing, and limited serviced land supply. More than 1 billion people already live in informal settlements (UN-Habitat, 2025), and the conditions that produced those settlements, including constrained land markets, limited institutional capacity, and low household incomes, remain largely unchanged.

The tendency for informal and low-quality housing to concentrate in hazard-prone areas is not incidental. It reflects the logic of land markets that systematically exclude low-income households from safe, well-serviced locations, directing them instead toward floodplains, steep slopes, coastal zones, and seismically active areas that formal markets have rejected precisely because of their risk profiles. Empirical evidence confirms this pattern across regions: informal settlements and substandard housing are disproportionately located in areas of high hazard exposure (Dodman et al., 2022; Rentschler et al., 2022). As long as the underlying conditions driving informal settlement persist, new housing demand will continue to be absorbed in these same locations. This pattern follows the standard logic of disaster risk: informal construction in hazard-prone areas increases exposure, while poverty and limited access to insurance or savings constrain coping capacity, compounding vulnerability and producing higher overall risk.

The cost of this overlap is substantial and growing. According to the 2025 Global Assessment Report (GAR): Resilience Pays: Financing and Investing, annual disaster costs now exceed $2.3 trillion when cascading and ecosystem losses are included (United Nations Office for Disaster Risk Reduction, 2025). A significant portion of these costs is attributable to housing losses. Building quality is a central factor: a large share of the existing stock was built without adherence to building codes, without technical oversight, and with materials that perform poorly under hazard stress (World Bank et al., 2025). Households in inadequate housing are more exposed to hazard events, suffer greater losses when events occur, have fewer resources for recovery, and are more likely to rebuild in the same hazardous locations (Hallegatte et al., 2016). Without a shift in the conditions governing where and how housing is built, this cycle will continue to generate disaster damage and losses at scale.

The body of research on housing and disaster risk has established a robust historical baseline. Studies document that 82 percent of new high-risk settlements between 1985 and 2015 occurred in low- and middle-income countries (Rentschler et al., 2023), and that the population exposed to floods alone increased by 20 to 24 percent between 2000 and 2018 (Tellman et al., 2021). What these studies do not address is the forward-looking dimension: where housing will be built, at what quality, and under what hazard conditions through the end of this century, and across the full range of relevant hazards including

earthquakes, tropical storms, and extreme heat. This gap has been partly a data limitation. Until recently, spatially explicit population projections at fine resolution beyond 2030 were unavailable. The release of the GHSL World Urbanisation Prospects (GHS-WUP) and FuturePop datasets now provides 1 km grid projections through 2100 under multiple SSP scenarios, making this analysis tractable. These datasets provide population and demographic projections, not housing projections directly; converting population into housing units requires the household size and cohort survival modelling described below. Building on these data, this study addresses three gaps in prior work in order to understand how future housing demand, hazard exposure, and construction quality will jointly evolve at global scale: the lack of spatial disaggregation in housing projections; the absence of simultaneous integration of demographic, hazard, and building quality dynamics at global scale; and the poorly quantified long-term cost implications of alternative construction quality pathways. It further introduces a classification of countries facing a triple burden of acute housing demand, disproportionate hazard exposure, and limited fiscal capacity to finance resilient construction. These three factors are selected because together they determine whether a country can convert housing need into resilient housing supply: demand sets the scale of construction required, hazard exposure determines the stakes of building it poorly, and fiscal capacity determines whether resilient construction is financially attainable at all.

This study specifically answers the following five research questions:

1. Where and when will new housing be built globally through 2100?
2. What proportion of future housing will be located in natural hazard-prone areas, across earthquakes, floods, tropical storms, and extreme heat?
3. How do alternative building quality pathways affect long-term housing resilience and replacement needs?
4. What are the cost implications of business-as-usual versus resilient construction?
5. Which countries face a convergence of high housing demand, severe hazard exposure, and limited fiscal capacity, and what does this imply for international policy support?

Together, these questions provide a global, forward-looking picture of where housing risk will concentrate and where resilient construction support is most urgently needed.

2. Data

The analysis integrated multiple globally comprehensive datasets spanning demographic projections, housing characteristics, and natural hazard indicators. All spatial data were harmonized to a common Mollweide equal-area projection (ESRI:54009) at 1km resolution to ensure consistent spatial calculations across diverse data sources.

Demographic Data

Population Projection: The study utilized two complementary sources for spatially explicit population projections. The Global Human Settlement Layer (GHSL) from the European Commission's Joint Research Center provides population grids for multiple time horizons based on historical settlement patterns and demographic models (Schiavina et al., 2026). WorldPop datasets offer alternative population projections with different Shared Socioeconomic Pathway (SSP) scenarios (Bondarenko et al., 2025). Both datasets provide 1 km gridded population estimates in 5-year intervals from 2025 to 2100.

Household Size Data: The study used three complementary data sources to obtain the most disaggregated household size information available worldwide. The primary data came from the CORESIDENCE Database, Version 2. This database provides subnational-level household size estimates for 136 countries including 1,482 administrative units (Galeano et al., 2024). The second source was the national-level average household size estimates from the same database, which added 21 more countries to the list. The third source was the country-level household size estimates derived from United Nations demographic databases (United Nations Department of Economic and Social Affairs, 2022), which added 33 countries. For countries without household size information, the regional average, as defined by the World Bank region classification, was used.

Demographic Projections The Shared Socioeconomic Pathways (SSP) Scenario Database from the International Institute for Applied Systems Analysis (IIASA) provides tabular demographic projections, including population breakdowns by age group, for each country under five SSP scenarios through the year 2100 (Riahi et al., 2017).

Housing Data

Housing Quality and Cost: The Global Earthquake Model (GEM) Foundation's Global Exposure Model provides subnational building inventory data that characterizes the quality of residential buildings through a standardized taxonomy (Yepes-Estrada et al., 2026; Yepes-Estrada et al., 2023). This dataset is structured as a table at the subnational level, which was spatially joined to subnational administrative boundary polygons to enable geographic analysis. The World Bank's Unbreakable study further classifies housing stock into three quality tiers (fragile, median, and robust) based on structural characteristics and construction materials (Middelanis et al., 2025).

Boundary and Economic Data

Administrative Boundaries: The country and first-level administrative boundaries were derived from the World Bank's Global Administrative Database. This database provides standardized vector geometries for 244 countries and territories (World Bank, 2025). These

boundaries were processed in the ESRI:54009 projection and rasterized to create a master grid template. This template enables consistent aggregation from 1-km pixel-level calculations to administrative units.

GDP and Urbanization Projection: The SSP Scenario Database from the IIASA provides GDP and urbanization projections for each of the five SSP scenarios up to the year 2100 (Chen et al., 2022).

Natural Hazard Data

This study constructed spatially explicit binary hazard masks for four natural hazards (flood, earthquake, tropical cyclone wind, and extreme heat) at 1 km^2 resolution aligned to the master population grid. Each hazard was assessed at a primary threshold representing meaningful structural or health risk to residential buildings, with a stricter secondary threshold used as a sensitivity check to test whether results are robust to a more conservative definition of hazard exposure.

Flood Hazard: Flood exposure was characterized using the World Resources Institute Aqueduct Flood Hazard Maps version 2 (World Resources Institute, 2020), accessed through Google Earth Engine. The dataset provides gridded projections of riverine and coastal inundation depth at approximately 1 km resolution across multiple return periods and climate scenarios. This study extracted 100-year return period flood depth projections for 2030, 2050, and 2080 under two climate forcing scenarios: RCP 4.5 and RCP 8.5. For riverine flooding, projections represent the ensemble mean across four general circulation models: NorESM1-M, GFDL-ESM2M, HadGEM2-ES, and IPSL-CM5A-LR. For coastal flooding, projections adopt the median sea level rise trajectory with land subsidence incorporated. The two components were merged at the pixel level by taking the maximum inundation depth, in order to produce a single composite flood exposure measure suitable for a global, multi-hazard comparison alongside earthquake, storm, and heat hazards. Grid cells with projected inundation depth exceeding 0.15 meters were classified as flood-prone. A secondary threshold of 0.5 meters was applied as a sensitivity check.

For the housing projection scenarios, SSP1 and SSP2 were paired with RCP 4.5, while SSP3, SSP4, and SSP5 were paired with RCP 8.5. Flood hazard layers are matched to housing projection years using the nearest available time slice: the 2030 layer is applied to projection years 2025 and 2030, the 2050 layer to 2040 and 2050, and the 2080 layer to 2060 through 2100. This analysis does not separately capture pluvial flooding, which can affect urban areas independently of river or coastal proximity. As a result, flood exposure in this study, particularly in dense urban areas, may be understated. Incorporating pluvial flood hazard is an area for future refinement as higher-resolution global datasets become available.

Seismic Hazard: Earthquake exposure was characterized using GEM's Global Seismic Hazard Map, which provides peak ground acceleration (PGA) with a 10 percent probability of being exceeded in 50 years return period at approximately 10 km resolution (Johnson et al., 2023). Grid cells where PGA exceeds 0.2g were classified as earthquake hazard zones, where structural damage becomes probable for non-engineered construction. A secondary threshold of 0.4g, associated with severe structural damage, was used as a sensitivity check.

Storm Hazard: Wind hazard from tropical cyclones was assessed using the STORM tropical cyclone wind speed return period datasets version 4 (Nadia Bloemendaal et al., 2023; Nadia; Bloemendaal et al., 2023). The dataset provides 100-year return period maximum sustained 10-minute wind speeds at approximately 10 km resolution. Two temporal layers were used. For projection years 2025 and 2030, the historical baseline layer is applied. For 2040 onwards, a future wind speed layer representing conditions at approximately 2050 was constructed by computing the pixel-wise ensemble mean across four models: CMCC-CM2-VHR4, CNRM-CM6-1-HR, EC-Earth3P-HR, and HadGEM3-GC31-HM. Grid cells with projected wind speeds exceeding 33 m/s (corresponding to Category 1 hurricane equivalent sustained winds) were classified as exposed to storm hazard. A secondary threshold of 42 m/s, broadly corresponding to Category 2 hurricane equivalent sustained winds, was applied as a sensitivity check.

Extreme Heat Hazard: Heat hazard was assessed using the NEX-GDDP-CMIP6 climate projection (approximately at 25km resolution), accessed through Google Earth Engine. Daily near-surface air temperature and relative humidity outputs from five models (GFDL-ESM4, IPSL-CM6A-LR, MPI-ESM1-2-HR, MRI-ESM2-0, and UKESM1-0-LL) were processed for two climate scenarios: SSP2-4.5 and SSP5-8.5. The heat metric used was the indoor wet-bulb globe temperature (WBGT) of the hottest calendar month within a decadal window centered on each projection year. Indoor WBGT was estimated using the formula:

$$WBGT_{indoor} = 0.7 \times T_w + 0.3 \times T_a$$

where T_w is the psychrometric wet-bulb temperature derived from air temperature and relative humidity following (Stull, 2011), and T_a is dry-bulb air temperature.

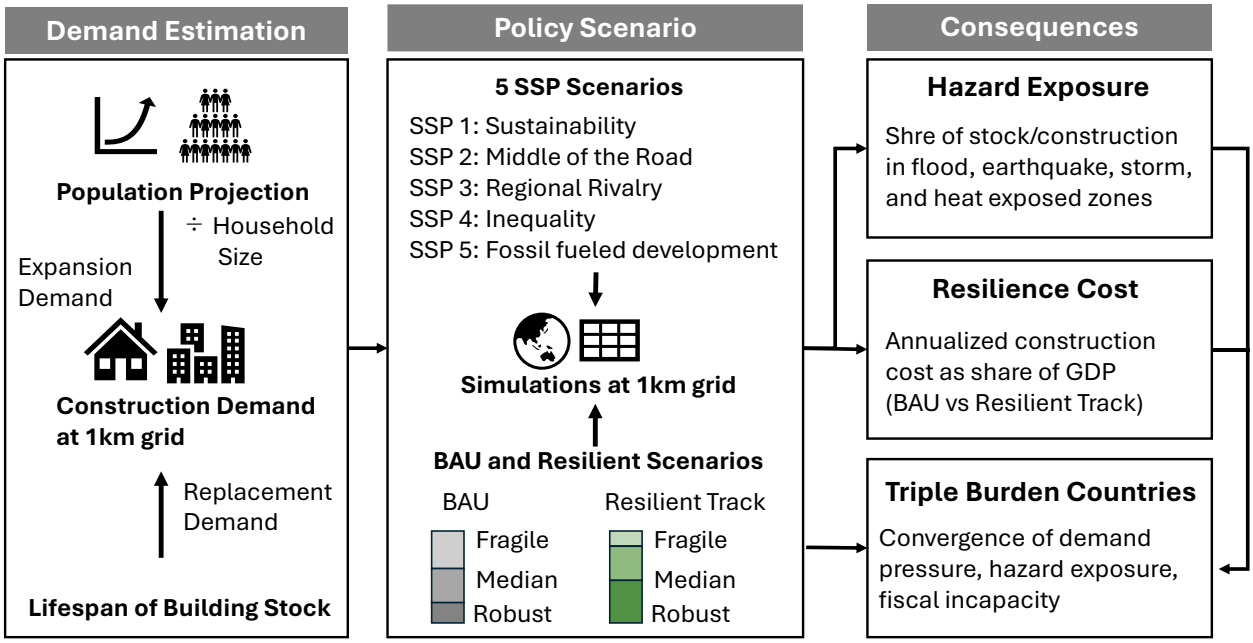
Monthly mean Indoor WBGT was computed for each model across each decadal window. For example, data from 2035 to 2044 were used for the 2040 projection year. For 2100, data from 2095 to 2100 were used given the data unavailability beyond 2100. Then, the hottest-month mean WBGT was averaged across the five models to produce a single estimate for each SSP scenario and projection year. This metric captures chronic heat stress in indoor residential environments during the peak seasonal period, which is directly relevant to

habitability and labor productivity in housing without mechanical cooling. Grid cells where the hottest-month indoor WBGT exceeds 32°C were classified as extreme heat hazard zones. A secondary threshold of 35°C was applied as a sensitivity check. SSP1 and SSP2 use the SSP2-4.5 heat projections, and SSP3, SSP4, and SSP5 use the SSP5-8.5 projections.

3. Empirical Approach

The analytical framework consists of six sequential stages (Figure 1). Each stage builds upon the previous stage's outputs to generate progressively refined projections of global housing stock evolution, structural quality, and replacement costs under alternative demographic and policy scenarios.

Figure 1 Analytical Framework



Stage 1: Econometric Projection of Household Size

The first stage projected average household size (AHS) for every 10 years through 2100. AHS governs the translation of population counts into housing units and is the key parameter linking demographic change to housing requirements. AHS is modeled using pooled ordinary least squares (OLS) regression on a cross-sectional, time-series dataset of country-level observations, with the natural logarithm of AHS as the dependent variable:

$$\ln(S_{j,t}) = \beta_0 + \beta_1 \ln(GDP_{i,t}) + \beta_2 U_{i,t} + \beta_3 C_{i,t} + \beta_4 E_{i,t} + \epsilon_{j,t}$$

where $S_{j,t}$ is the average household size in geographic unit j (country or subnational area)at time t; $\ln(GDP_{i,t})$ is the natural log of GDP per capita (PPP), proxying economic

development and the affordability of independent household formation; $U_{i,t}$ is the urbanization rate, capturing the structural shift from multi-generational rural households toward smaller urban units; $C_{i,t}$ and $E_{i,t}$ are the shares of the population aged 0–14 years and 65 years or older, respectively. Country-level covariates are used when subnational household-size observations are available for unit j within country i. These covariates represent socioeconomic development, urbanization and demographic composition, which are associated with household size across countries and over time.

Country-specific factors such as cultural norms, housing policies, and tenure arrangements are not fully captured by the included covariates. A standard response is to introduce country fixed effects. However, for projections extending to 2100, country fixed effects identify coefficients exclusively from within-country temporal variation over a short historical window. This is appropriate for short-run forecasting but not for long-run structural projection, where the cross-country gradient is the primary signal guiding trajectories for countries expected to undergo significant economic and demographic transformation. As reported in Annex 2, the OLS coefficients closely track the between-country (cross-sectional) effects. A random slopes multilevel model further supports the assumption of a globally homogeneous slope. A full four-way robustness comparison across OLS, country fixed effects, between-effects, and correlated random effects specifications is presented in Annex 2.

To address spatial heterogeneity, this study computed an area-specific offset (δ_j) for each subnational unit or country j, defined as the residual between observed and model-predicted log AHS at the base year closest to 2025:

$$\delta_j = \ln\left(S_{j,\text{obs}}\right) - \ln\left(\hat{S}_{j,\text{base}}\right)$$

This offset is equivalent to a unit-specific fixed intercept, but anchored to observed subnational data where available, providing finer spatial resolution than a country-level fixed effect. Where subnational survey data exist, δ_j was computed for each subnational unit. Where only national data are available, δ_j was computed at the country level. For countries with insufficient data, offset factors were imputed from World Bank regional averages. It is acknowledged that the offset is held fixed throughout the projection period, which becomes a stronger assumption at longer time horizons.

Future AHS was then projected as:

$$\hat{S}_{j,\text{t}} = \exp\left(f\left(X_{i,t}\right) + \delta_j\right)$$

All projections were bounded between the 1st and 99th percentiles of the historical AHS distribution to prevent implausible extrapolation.

Stage 2: Spatial Framework and Housing Stock Estimation

The second stage translated demographic projections into spatially explicit housing stock requirements at 1km^2 resolution. AHS projections were rasterized to match the gridded population dataset, with a Euclidean distance transform and nearest-neighbor assignment ensuring that every populated grid cell has a corresponding AHS value. The required housing stock (H) for each grid cell k in area j at year t is:

$$H_{k,j,t} = \frac{P_{k,j,t}}{\hat{S}_{j,\mathrm{t}}}$$

where $P_{k,j,t}$ is the projected population and $\hat{S}_{j,\mathrm{t}}$ is the projected Average Household Size.

The use of households as proxies for dwelling units follows the established practice of the housing needs literature. For example, the methodological basis for the widely cited UN-Habitat demand estimates of 96,000 housing units per day uses households as proxies for housing units(UN-Habitat, 2005). This approach assumes household size is relatively uniform within subnational boundaries, which is a reasonable approximation given data constraints, though urban-rural differences in household size represent a limitation that future research could address.

Stage 3: Dynamic Cohort Survival and Housing Quality Evolution

The third stage used a recursive dynamic cohort survival model to track the evolution of housing stock quality and construction volumes from 2025 through 2100 across three structural quality tiers: Fragile, Median, and Robust. Initial quality distributions were derived from the Global Exposure Model. The nighttime population attribute in GEM served as a proxy for occupied dwellings, and the proportional shares of fragile, median, and robust stock were computed for each subnational region and disaggregated to the 1 km^2 grid. The model advanced in five-year steps for year 2025-2030 and ten-year steps for the remaining projection period, where n denotes the length of each simulation interval in years.

For each simulation step, the gross construction requirements (C_{total}) were calculated by comparing the target housing demand against the surviving building stock. This requirement was decomposed into two analytically and economically distinct components:

1. **Expansion Demand (C_{exp})** represents the net addition to the housing stock required solely by demographic pressure:

$$C_{exp,k,t} = \max\left(0, H_{target,k,t} - H_{total,k,t-n}\right)$$

2. **Replacement Demand (C_{rep})** represents the construction needed to replace depreciated units to maintain the required stock level. Existing stock depreciates based on quality-specific lifespans (L_q): 20 years for the Fragile tier, 40 years for the Median tier, and 60 years for the Robust tier, reflecting empirical evidence from multiple regional contexts (See Annex 1 for details). The surviving stock at each step is:

$$V_{k,t} = \sum_{q} \left[H_{q,k,t-n} \times \left(1 - \frac{n}{L_q}\right) \right]$$

Total and replacement construction requirements follow as:

$$C_{total,k,t} = \max\left(0, H_{target,k,t} - V_{k,t}\right)$$

$$C_{rep,k,t} = C_{total,k,t} - C_{exp,k,t}$$

In cells with declining demand, expansion demand is zero and replacement demand was capped at the number of depreciated units needed to maintain the lower target stock level.

The quality composition of new construction was determined by the policy scenario. Under the Business-as-Usual (BAU) scenario, new construction replicated the typology mix of the preceding stock, embedding structural inertia: regions with predominantly fragile housing continue to build fragile housing absent policy intervention. Under the Resilient Policy scenario, the lowest-quality tier was progressively phased out of new construction through a transition matrix applied to each new cohort:

- New Fragile Share: $0.5 \times \sigma_F$
- New Median Share: $(0.5 \times \sigma_F) + (0.5 \times \sigma_M)$
- New Robust Share: $(0.5 \times \sigma_M) + \sigma_R$

Where σ_F, σ_M, and σ_R denote the current shares of Fragile, Median, and Robust stock in the preceding cohort respectively.

This ensures that structural upgrading is gradual, with the pace governed endogenously by existing stock composition and replacement cycles. Alternative scenarios, consisting of higher governance and lower governance implementation capacities (75 percent upgrade and 25 percent upgrade, respectively), were tested as sensitivity analysis.

Stage 4: Hazard Exposure Assessment

The fourth stage overlaid dynamic housing stock projections with natural hazard layers to quantify physical exposure of housing units to climate-related and geophysical risks. All

hazard layers were resampled to the 1km^2 grid using nearest-neighbor interpolation to ensure pixel-level alignment.

Exposure was assessed across two dimensions. Stock exposure measured the total number of housing units located within hazard zones during each simulation period, disaggregated by structural quality tier, characterizing the accumulated physical risk in the built environment at a given point in time. Construction flow exposure isolated newly constructed units within hazard zones at each simulation step, revealing where development is actively expanding the risk frontier. This includes both densification within existing built-up areas, such as replacement of lower-density structures with higher-density ones, and greenfield development in areas not previously urbanized. Both pathways represent a meaningful increase in exposure, particularly when expansion occurs in flood-prone or otherwise hazard-affected locations.

To distinguish these two pathways, a threshold of 300 inhabitants per 1 km^2 grid cell was applied following established global urban-rural classifications (Dijkstra et al., 2021). Cells below this threshold were classified as candidates for greenfield development when net housing expansion was projected within them, with direct implications for land policy, cadastral planning, and land entitlement processes. Cells above the threshold were treated as existing built-up areas where densification contributes to construction flow exposure.

Stage 5: Affordability of Resilient Measures

The fifth stage translated physical construction projections into economic cost estimates and evaluated the fiscal feasibility of transitioning from BAU to resilient track. Unit replacement costs were derived from the GEM dataset at country level and adjusted for future periods using projected GDP per capita (PPP). Cumulative construction volumes by quality tier from Stage 3 were annualized by dividing period totals by the number of years in each simulation interval, and unit costs were then applied. Annualized costs were benchmarked against projected national GDP under each SSP scenario, expressed in PPP terms to facilitate cross-country comparison.

Stage 6: Triple Burden Classification

The sixth stage constructed a composite index to identify countries where three structural disadvantages converge simultaneously. Three indicators were derived from scenario model outputs: total projected housing unit requirements between 2025 and 2100 as a share of 2025 stock (demand pressure); the share of cumulative new construction located in high-risk zones across four hazard types (earthquake, flood, storm, and heat), capturing hazard exposure; and the peak annual incremental cost of resilient construction as a share

of GDP, capturing affordability constraints. Benchmarking incremental construction costs against GDP follows standard practice in the fiscal space literature, where a government's capacity to absorb a given spending obligation is assessed relative to the overall size of its economy (Kose et al., 2022).

Each of the three indicators was normalized using min-max scaling to place them on a common zero-to-one scale, removing differences in absolute magnitude across indicators and countries. For the hazard exposure indicator specifically, which aggregates across four distinct hazard types (earthquake, flood, storm, and heat), an additional normalization step was required: each hazard's raw exposure rate was first scaled to zero-to-one using min-max normalization, and the resulting scores were then converted to percentile ranks to equalize the distributional influence of each hazard type before they were averaged into a single hazard exposure score. For each indicator, the worst-case value across all six demographic scenarios (GHSL, SSP1-SSP5) was retained per country. The three worst-case scores were then normalized and averaged into an unweighted composite index across all countries. Countries in the top quartile were considered triple burden countries.

Sensitivity Analysis

The model was evaluated under three sensitivity dimensions alongside the baseline: building lifespan assumptions, governance implementation capacity, and natural hazard classification thresholds. All sensitivity runs used SSP3.

Building lifespan assumptions are among the most consequential parameters in the model, as replacement demand constitutes the majority of total global construction need throughout the projection horizon. Three parameter sets were evaluated: a short lifespan variant (Fragile = 10 years, Medium = 30 years, Robust = 50 years), the baseline (Fragile = 20 years, Medium = 40 years, Robust = 60 years), and a long lifespan variant (Fragile = 25 years, Medium = 50 years, Robust = 75 years).

Governance implementation capacity determines the rate at which newly constructed housing under the Resilient pathway meets higher quality standards. The baseline assumed moderate implementation (50 percent upgrades among new construction). Two alternative scenarios were evaluated: low implementation (25 percent upgrades, reflecting weak regulatory enforcement) and high implementation (75 percent upgrades, reflecting strong institutional capacity and enforcement).

Natural hazard thresholds define the exposure level at which a housing unit was classified as at risk. The baseline thresholds reflected moderate return-period events. A stricter second-threshold variant was evaluated using more severe exposure levels: heat stress at 35 degrees Celsius indoor wet-bulb global temperature equivalent, flood depth at 0.5

meters, wind speed at 42 meters per second, and peak ground acceleration at 0.4g for seismic hazard.

Model Validation

To assess the predictive accuracy of the household size projection model, the study applied a temporal hold-out validation approach that mirrors the full projection pipeline. This approach tests whether the model, when trained only on older data, can accurately predict outcomes it has not yet seen. The historical dataset is split at a cutoff year: observations before the cutoff are used to re-fit the model and compute offsets, while observations from the cutoff onward are set aside and used only to check the model's predictions against actual outcomes, rather than being used in the fitting process itself. The validation covers both subnational and national units following the same hierarchy used in the projection: subnational units are validated where subnational data exist on both sides of the cutoff, and national-level units cover the remaining countries. The study uses 2005 as the primary cutoff, providing a hold-out window of approximately 17 years, and 2008 as a secondary cutoff to test robustness.

4. Results

This section presents results in six parts, following the sequence of the empirical approach. It begins with the household size regression that underlies the translation of population into housing units, then presents global and regional housing stock trajectories through 2100. It next decomposes construction demand into expansion and replacement components and compares outcomes under Business-as-Usual and Resilient construction pathways. The section then examines the exposure of current and future housing stock to natural hazards, followed by the cost implications of resilient construction and its fiscal affordability across regions. It concludes with the triple burden classification of countries facing convergent demand, hazard, and affordability pressures, and a summary of sensitivity and model validation results.

Drivers of Household Size Dynamics

The estimated regression coefficients in Table 1 reveal the direction and magnitude of each driver's contribution. The negative coefficient on log GDP per capita indicates that, as countries become wealthier, average household size declines. This pattern is consistent with theories of household nuclearization and greater affordability of independent living arrangements. Age structure emerges as a particularly influential set of determinants. A higher percentage of children aged 0–14 is associated with larger households. In contrast, a higher percentage of elderly individuals aged 65 and over is strongly and negatively associated with household size. This reflects the tendency toward fragmentation, including

single-person households, in aging societies. Once income and age structure are held constant, however, the independent effect of urbanization is small in magnitude and slightly positive. This suggests that the conventional association between urbanization and reduced household size is largely mediated by its correlation with income growth and demographic aging rather than representing an independent urban effect. Overall, the global econometric model has strong explanatory power, with an R^2 of 0.79.

The robustness analysis presented in Annex 2 provides additional support for this specification. The between-effects model, which isolates the cross-country structural gradient, produces coefficients that closely align with the pooled OLS estimates across all four regressors, confirming that OLS captures the relevant long-run signal.

Table 1 Global Model Coefficients (N = 984)

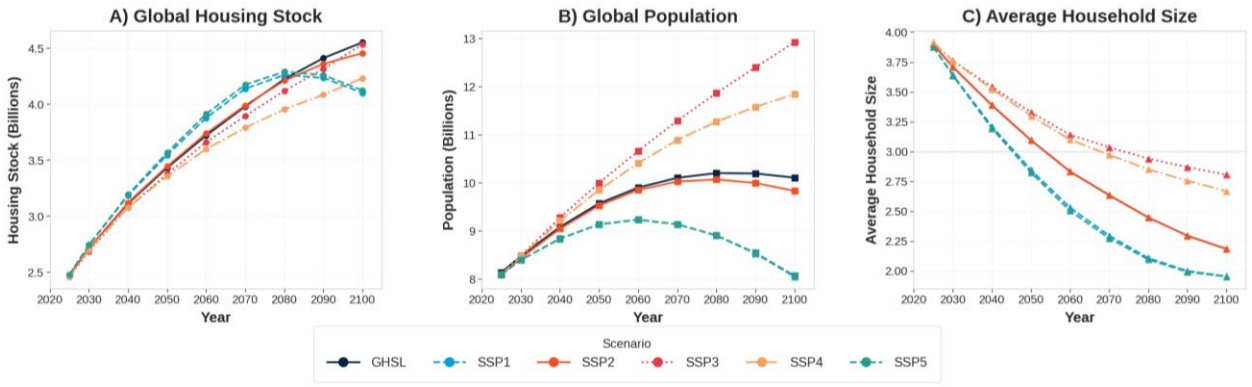
Variable	Coefficient	Interpretation
Intercept	1.8230	Baseline constant
Log (GDP per capita)	-0.0594 ***	Wealthier populations form smaller households
Urban Rate	0.0005	Marginal effect after controlling for income and age
Child Rate (0-14)	0.0087 ***	Higher child share associated with larger households
Elderly Rate (65+)	-0.0266 ***	Aging populations associated with household fragmentation

*Note: *** $p < 0.01$. Standard errors clustered by country. Full model statistics are reported in Annex 2.*

Global Housing Stock Trajectories (2025–2100)

Translating these demographic dynamics into housing unit requirements (Stage 2) reveals striking differences in the projected global demand for housing across various scenarios. Figure 2 shows the trajectories of global housing stock, population, and average household size under GHSL and five SSPs.

Figure 2 Global Housing Stock, Population, and Household Size Trajectories (2025-2100)



All scenarios begin from a common 2025 baseline of approximately 2.46 billion to 2.48 billion housing units. By 2100, total global housing stock is projected to nearly double

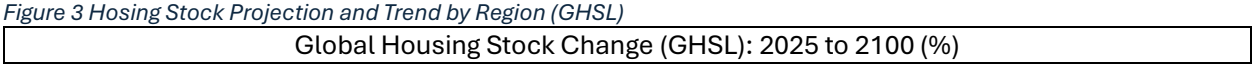
across all scenarios, reaching between 4.10 billion units (SSP1) and 4.55 billion units (GHSL), representing growth of 65% and 84%, respectively, relative to the 2025 baseline.

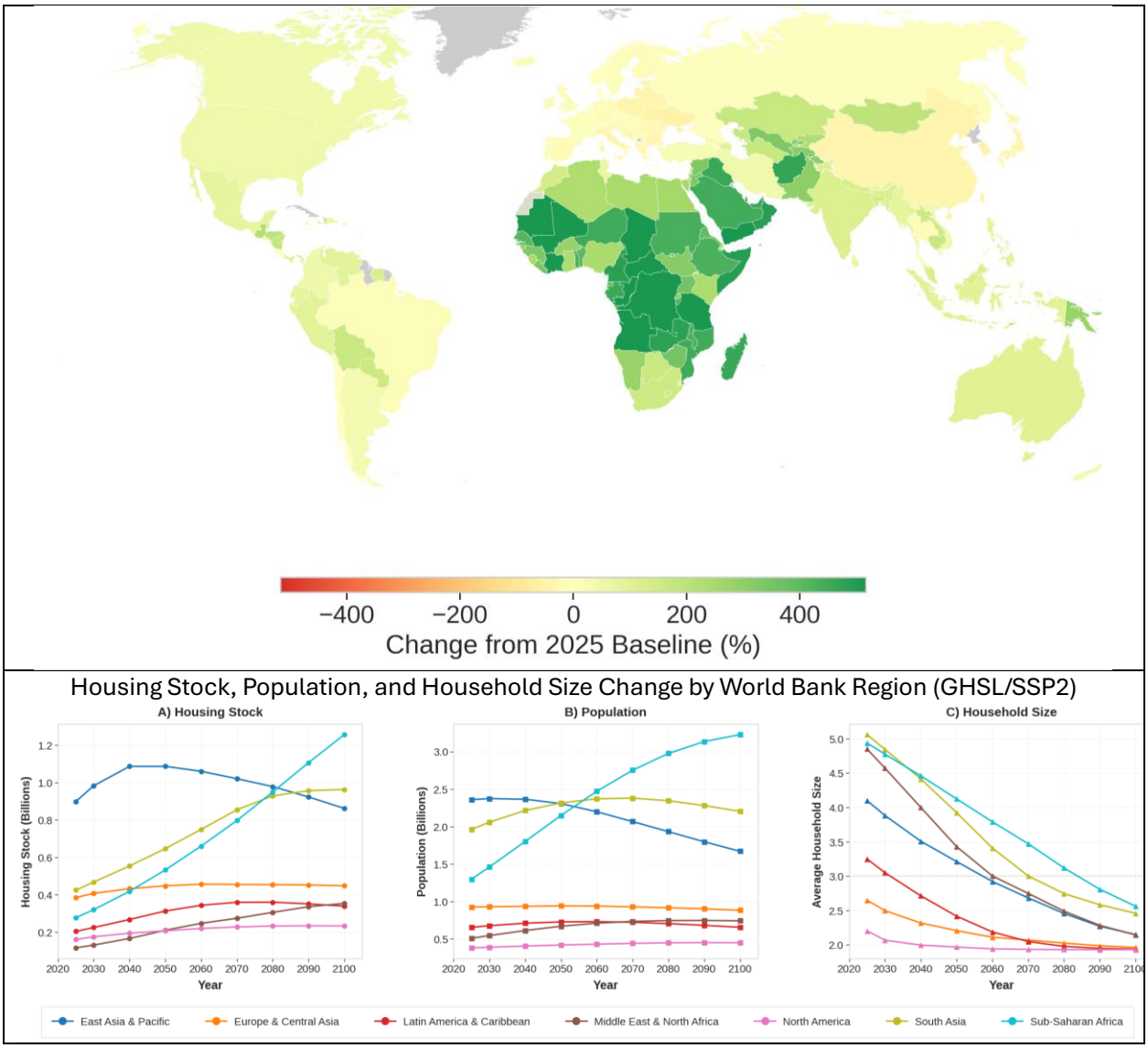
A comparison of SSP3 (Regional Rivalry) and SSP5 (Fossil-fueled Development) illustrates a fundamental decoupling of population growth from housing demand. By 2100, the global population under SSP3 is projected to reach approximately 12.9 billion, compared to a peak-and-decline trajectory under SSP5 that settles at approximately 8.1 billion, a difference of nearly 4.8 billion people. Despite this substantial demographic divergence, the required housing stock across the two scenarios converges to a remarkably similar magnitude: an estimated 4.53 billion units under SSP3 (BAU) versus 4.12 billion under SSP5 (BAU). This gap of only 400 million units, or less than 10%, is notably small given a population difference of 60%.

This result reflects the elasticity of household size with respect to economic development. Under SSP3, slower economic growth delays the demographic transition, keeping average household sizes comparatively large throughout the century. As a result, the much larger population is accommodated primarily through higher household density rather than a proportional expansion of the housing stock. Under SSP5, by contrast, rapid economic growth and urbanization drive a pronounced reduction in average household size. As a result, despite a substantially smaller total population, the fragmentation of households sustains a comparably high aggregate demand for housing units.

Figure 3 presents the projected percentage changes of housing stock, with regional trend of housing stock, population, and household size trajectories from 2025 to 2100, using the GHSL scenario for stock and SSP2 for population and household size. The analysis reveals stark regional divergences that will fundamentally reshape global housing demand over the coming decades.

Figure 3 Hosing Stock Projection and Trend by Region (GHSL)





Sub-Saharan Africa exhibits the most pronounced growth trajectory across all three dimensions. Housing stock in the region is projected to expand nearly five-fold from 2025 levels, approaching 1.12 billion to 1.37 billion units by 2100, driven simultaneously by rapid population growth and persistent, though gradually declining, household sizes. The Middle East and North Africa region is projected to experience 167 to 225 percent growth in housing stock, followed by South Asia, where the upward trajectory continues through 2100 but at a decelerating pace from approximately 2080 onward, resulting in cumulative growth of 105 to 144 percent.

In stark contrast, East Asia and the Pacific, currently the region with the largest housing stock at approximately 0.9 billion units, is projected to peak around 2040 before entering a gradual but sustained decline. This trajectory reflects the convergence of population aging, low fertility, and already-advanced household size reduction. Latin America and the

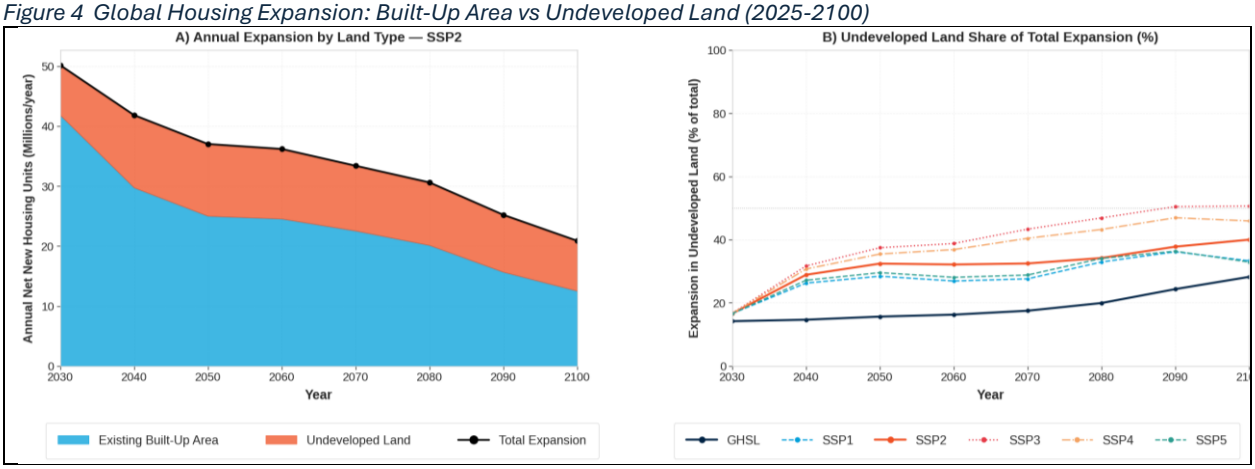
Caribbean occupy an intermediate position, exhibiting moderate and steady growth throughout the period.

Europe and Central Asia present a qualitatively distinct challenge. While aggregate housing stock shows near-zero net growth, this apparent stability masks a substantial need for replacement construction as the existing stock ages and becomes functionally obsolete. The region faces falling demand for new unit construction while simultaneously confronting the financial and logistical burden of stock renewal. This dynamic is structurally different from the expansion challenge facing high-growth regions and warrants dedicated policy attention.

Expansion Demand versus Replacement Demand

Figure 4 shows the trend in new housing expansion demand, driven purely by population increase and household size shrinkage. It does not include replacement demand, which is discussed below. Across all scenarios, annual expansion demand follows a consistent long-run trajectory: it peaks in the 2025–2030 period and then declines gradually toward 2100 as demographic growth moderates. SSP1 and SSP5 yield high early-century expansion of approximately 54 million units per year, reflecting their faster initial household fragmentation. By the 2090–2100 decade, annual expansion requirements will fall sharply: to approximately 10 million units per year under SSP1 and SSP5, approximately 21 million per year under SSP2, approximately 26 million per year under SSP3, and approximately 27 million per year under the GHSL projection. It is also important to note that around 20% to 50% of expansion demand is happening in the areas undeveloped today, underscoring the importance of front-loading infrastructure investment. Figure A5-1 (Annex 5) provides regional annual housing expansion in existing built-up versus undeveloped land.

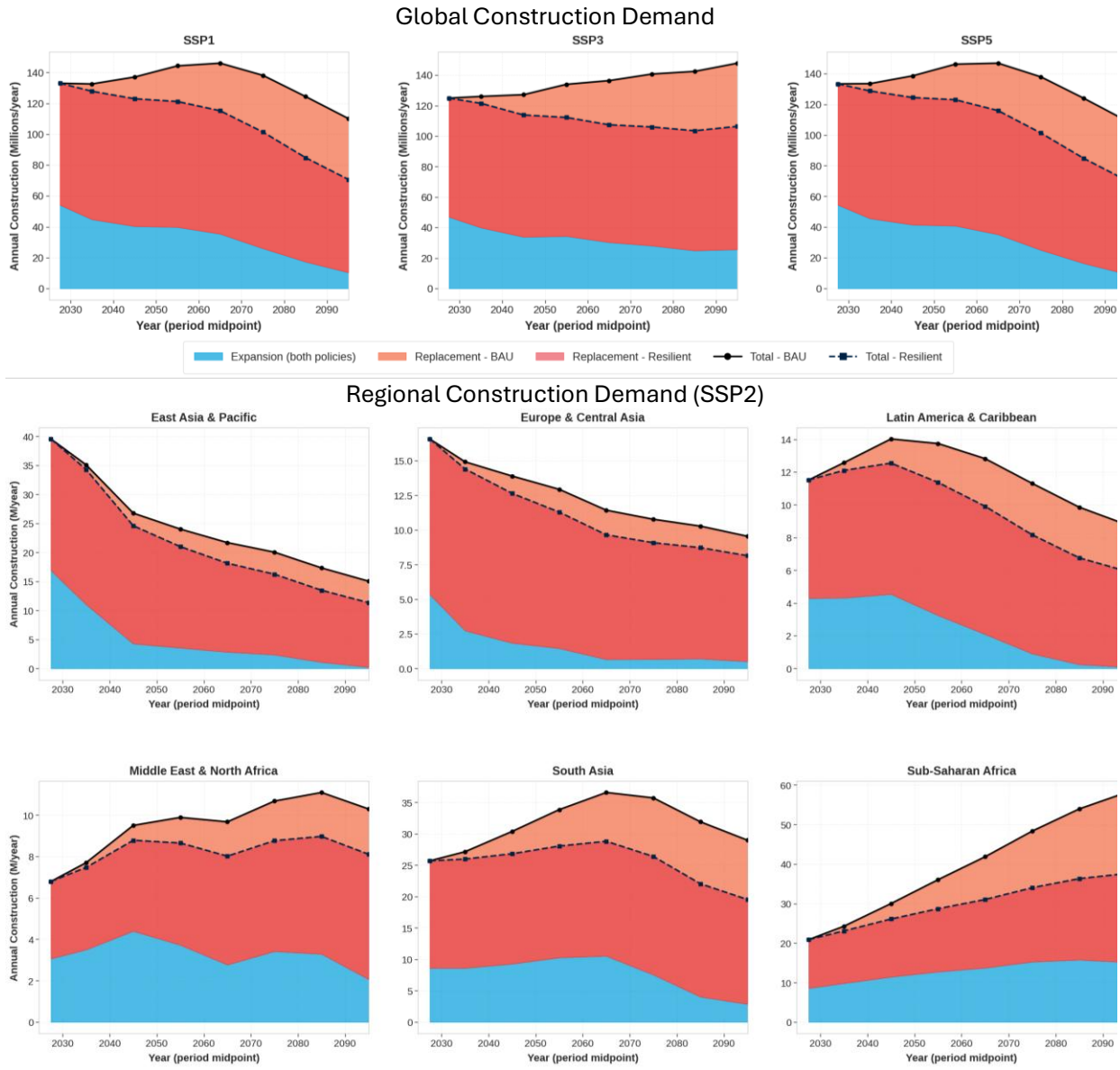
Figure 4 Global Housing Expansion: Built-Up Area vs Undeveloped Land (2025-2100)



While housing expansion is driven by population increase and household decomposition, housing replacement requirements are determined by the quality and age of the existing

housing stock. Figure 5 decomposes global and regional annual housing construction demand into its two constituent components, expansion and replacement, across three demographic scenarios (SSP1, SSP3, and SSP5) for global comparison and SSP2 for regional, contrasting Business-as-Usual (BAU) and Resilient policy pathways from 2025 to 2100. The results illuminate critical differences in construction timing, volume, and the long-term returns to quality-focused housing investment.

Figure 5 Global and Regional Construction demand: BAU vs Resilient Policy (SSP1, 3, 5 for Global; SSP2 for Regional)



The expansion component, shown in light blue and representing demand from net household formation and population growth, is identical across both policy pathways and declines continuously over the projection horizon. The replacement component, which reflects the need to rebuild or renew deteriorating housing stock, diverges substantially

between the two pathways. Under the BAU pathway, replacement demand escalates progressively as the large volumes of fragile stock built during the early and mid-century reach the end of their service lives. By the 2090–2100 decade, annual replacement demand under BAU ranges from approximately 100 million units per year (SSP1) to approximately 122 million units per year (SSP3), with the GHSL projecting 118 million units per year. Under the Resilient pathway, where new units are built to higher durability standards and therefore carry longer functional lifespans, replacement demand in the same terminal decade falls to approximately 60 million units per year (SSP1), 74 million (SSP2 and GHSL),and 80 million (SSP3). This represents a 34–40% reduction in annual replacement requirements relative to BAU.

Looking at the trend by region, Sub-Saharan Africa shows a continued increase in new housing construction, with a growing share built on previously undeveloped land (Annex Figure A5-1). In South Asia and Latin America and the Caribbean, annual housing demand is projected to be slightly lower in the 2050 period compared to 2030, but the proportion of new housing built on undeveloped land is expected to increase. Similar trends are observed in the Middle East and North Africa and North America, where the share of new housing on undeveloped land rises toward 2100. East Asia and the Pacific shows a large proportion of construction on undeveloped land in the early period, declining over time, which points to the importance of taking immediate action.

Taken together, these results point to a fundamental structural transition in the composition of global housing construction activity. During the early part of the century (2025–2050), slightly less than half of construction is still expansion-driven, requiring greenfield development and the extension of urban infrastructure into new areas. By the latter part of the century (2070–2100), construction becomes increasingly replacement-dominated, shifting the challenge toward urban renewal and stock management. The Resilient policy pathway reshapes this transition materially, reducing late-century replacement burdens through front-loaded investment in housing quality and durability. As illustrated in Figure 6, the share of fragile housing in the total stock declines substantially more rapidly under the Resilient scenario than under BAU, across all SSP scenarios examined.

Figure 6 Housing Quality Composition: BAU vs Resilient Policy Scenarios (GHSL)

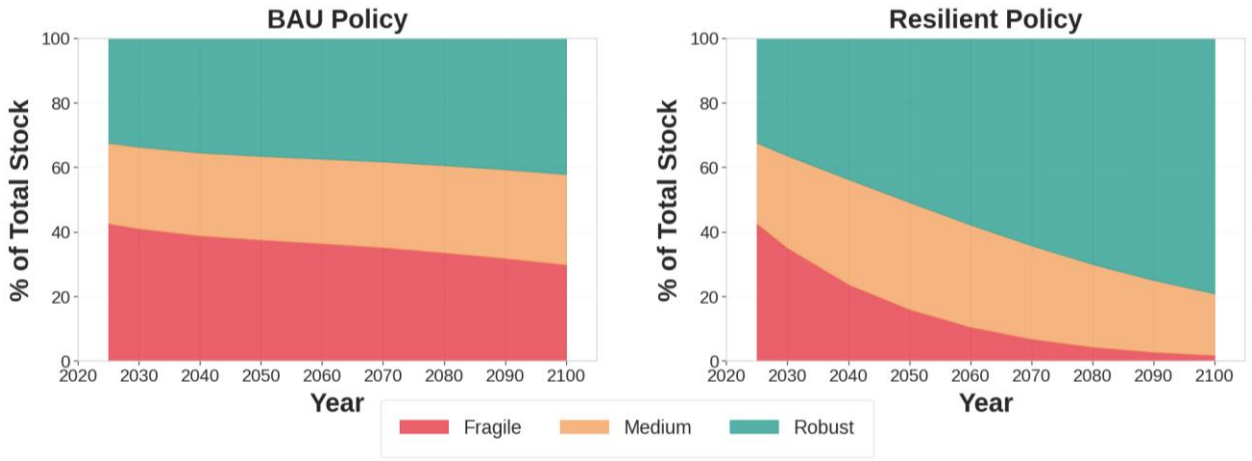
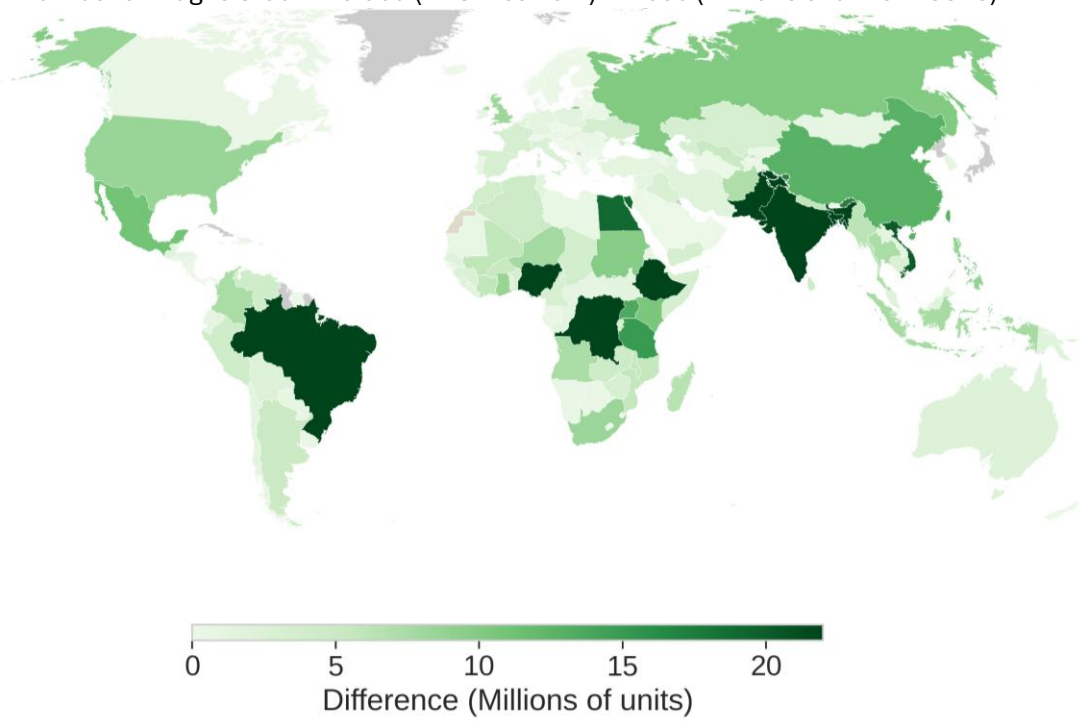


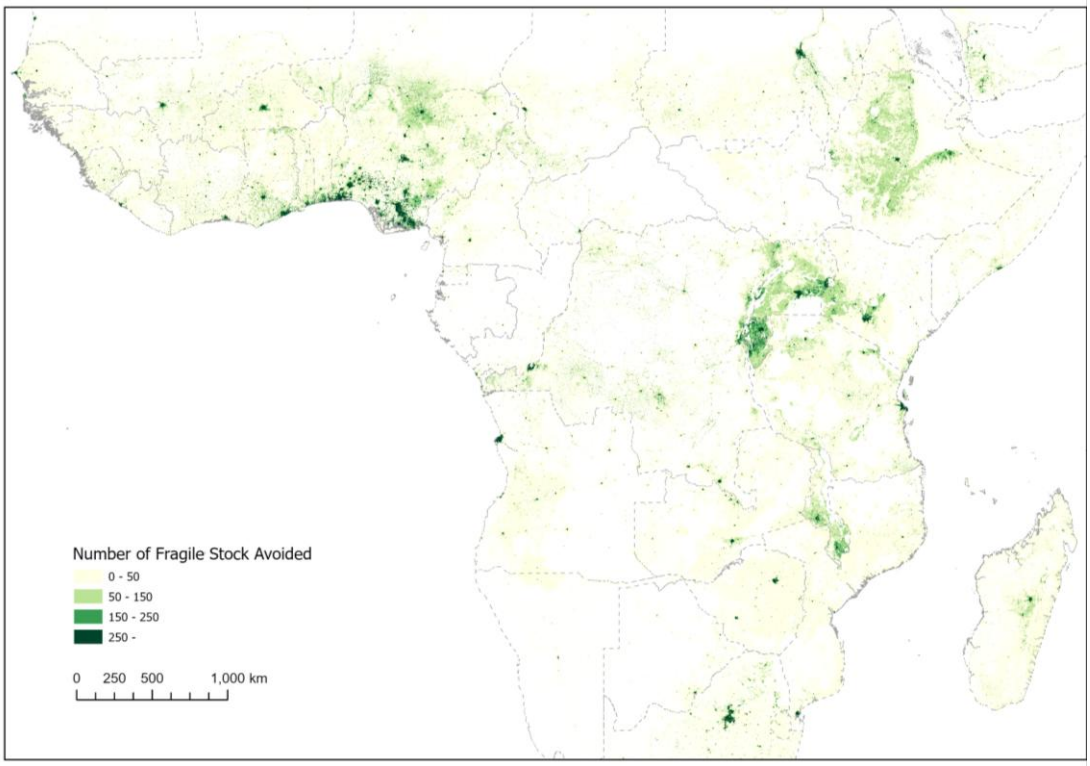
Figure 7 maps the spatial distribution of avoided fragile housing units attributable to resilient policy, calculated as the difference between the BAU and Resilient scenarios in 2050 under SSP3. In the bottom map focused on Sub-Saharan Africa, the areas shaded in dark green indicate high policy dividends, defined as locations where more than 250 fragile housing units per km^2 are avoided through resilience investments. Major dividend hotspots are concentrated along the southern coast of West Africa, encompassing Nigeria, Ghana, Togo, and Benin, as well as in the densely populated inland areas of Burundi and Rwanda, and in major urban centers including Nairobi, Dar es Salaam, Luanda, Kinshasa, Lusaka, Antananarivo, and Harare. These spatial patterns underscore the importance of geographically targeted policy implementation, as the returns to resilience investment are highly concentrated rather than uniformly distributed. This aligns with evidence that African cities are expanding at some of the fastest rates globally, with urban land conversion outpacing population growth (Güneralp et al., 2017), creating an urgent window for risk-informed spatial planning.

Figure 7 Policy Dividend (SSP3) in Global (top) and Sub-Saharan Africa (bottom): Avoided Fragile Housing (2050)

Number of Fragile Stock Avoided (BAU-Resilient) in 2050 (Millions of units in SSP3)



Number of Fragile Stock Avoided (BAU-Resilient) in Sub-Saharan Africa at 1km grid in 2050 (SSP3)



Note: Map projection: Africa Albers Equal Area Conic (ESRI:102022). Data resolution: 1 km. Darker green = higher policy dividend.

Housing Expansion into Hazard-Exposed Areas

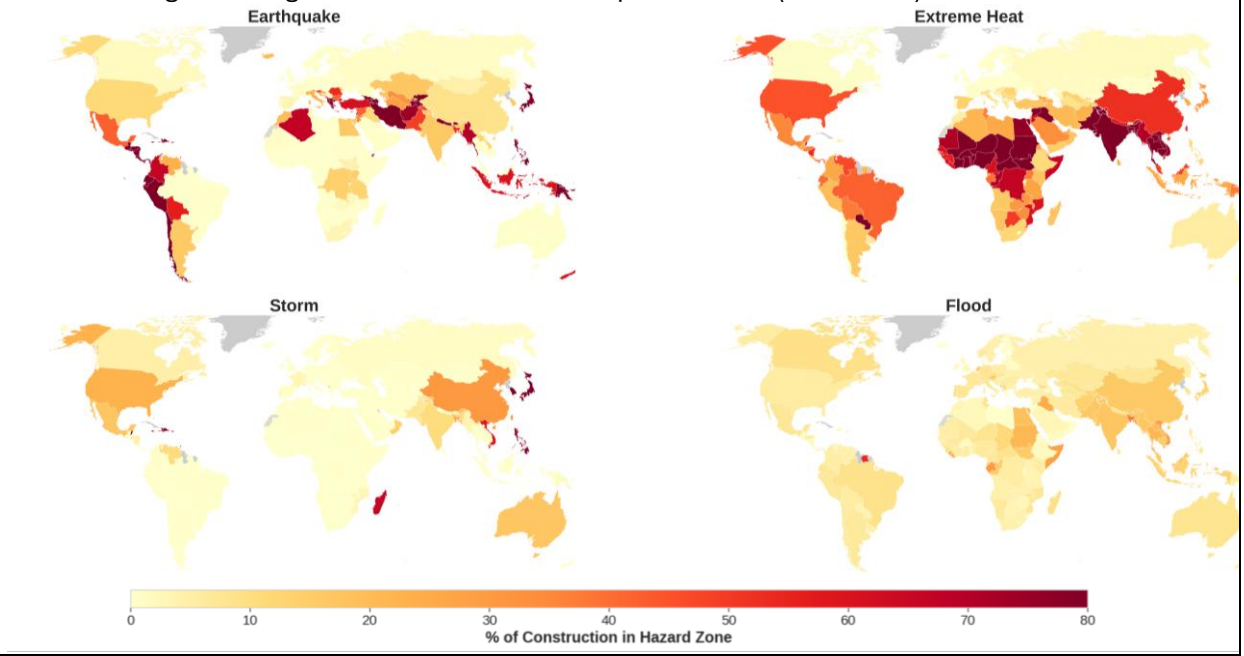
A substantial and growing share of housing construction is being concentrated in areas exposed to significant natural hazard risk (Figure 8 and Annex Figure A5-2). Between 2025 and 2100, the total number of housing units located in hazard-exposed areas is projected to increase substantially across all hazard categories and across all SSP scenarios. Flood-exposed housing stock grows from approx. 250 million units in 2025 to between 419 million and 513 million by 2100, an increase of 68 to 98 percent depending on the SSP scenarios. Earthquake-exposed stock rises from approximately 495 million to between 833 million and 932 million units, an increase of 67 to 88 percent. Storm-exposed stock grows more moderately, from approximately 364 million to between 472 million and 547 million units, an increase of 30 to 50 percent. Extreme heat exposure sees the most dramatic increase of any hazard category: heat-exposed housing stock grows from approximately 630 million units in 2025 to between 2.3 billion and 3.2 billion units by 2100, an increase of 267 to 412 percent. The wide ranges across SSP scenarios reflect differences in total population, urbanization trajectories, and climate scenarios, but the direction of change is consistent across all scenarios.

The regional breakdown of hazard exposure reveals important heterogeneity in risk trajectories. For earthquakes, East Asia and the Pacific currently has the largest exposed housing stock, though new seismic-zone construction in the region is on a declining trend. South Asia, by contrast, continues to increase new construction in seismically active areas at a rapid rate, signaling a growing divergence in future exposure. Similar patterns are observed for flood: new construction in flood-prone areas in South Asia and Sub-Saharan Africa is expanding, and these two regions are on course to account for a disproportionate share of global flood-exposed housing stock by mid-century. Extreme heat exposure in new construction is also concentrated most heavily in Sub-Saharan Africa and South Asia. Storm exposure remains highest in East Asia and the Pacific.

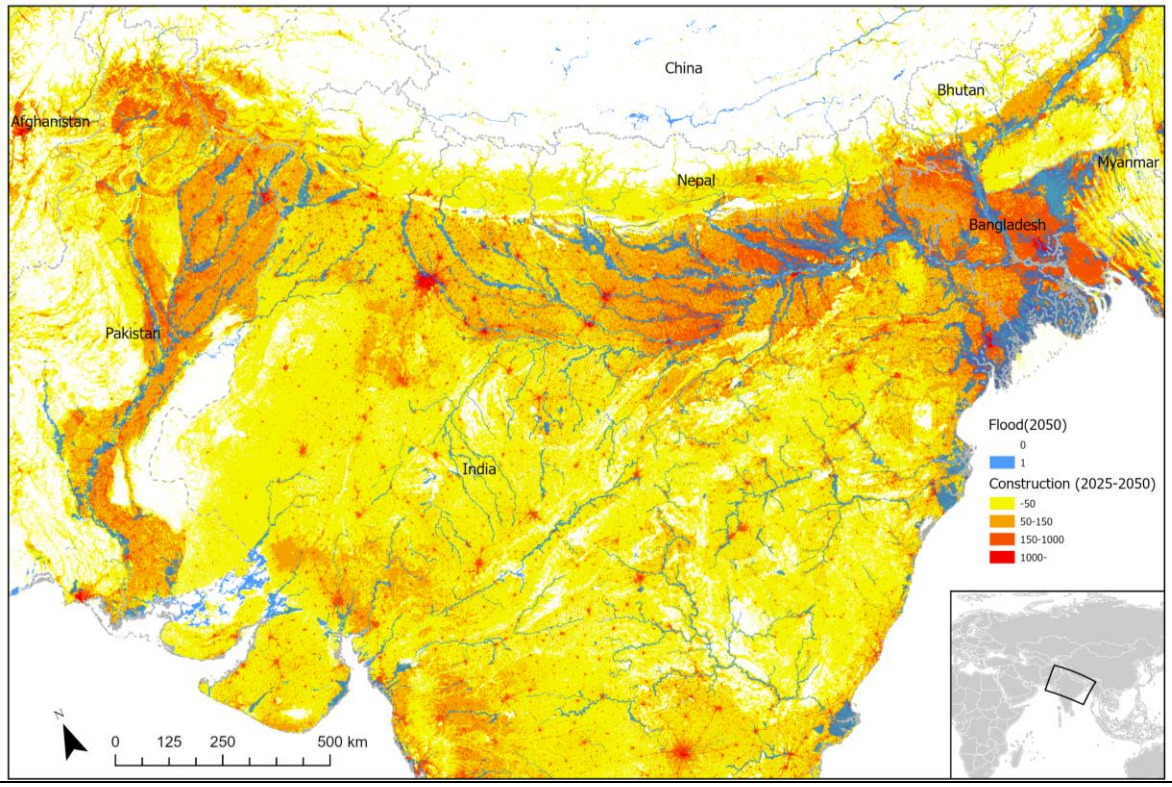
The bottom map in Figure 8 illustrates the spatial dimension of this risk accumulation in South Asia, mapping cumulative new construction projected for 2025–2050 under SSP3 BAU overlaid with flood hazard zones. High-risk concentrations (shown in red) indicate areas where more than 500 housing units per km^2 are being built. Notable hotspots include: (i) the Indus River basin in Pakistan, particularly Sindh and Punjab provinces; (ii) the Ganges–Brahmaputra delta in Bangladesh; and (iii) the Indo-Gangetic Plain across northern India. These regions face compounding and mutually reinforcing risks from riverine flooding, coastal storm surge, and rapid unplanned urbanization, a combination that renders the current trajectory of construction particularly consequential.

Figure 8 Hazard exposure of future housing construction (SSP3)

Annual Average Housing Construction in Hazard Exposed Zones (2025-2100) SSP3



Projected Flood Risk and Construction Activity (2025-2050), South Asia (SSP3)

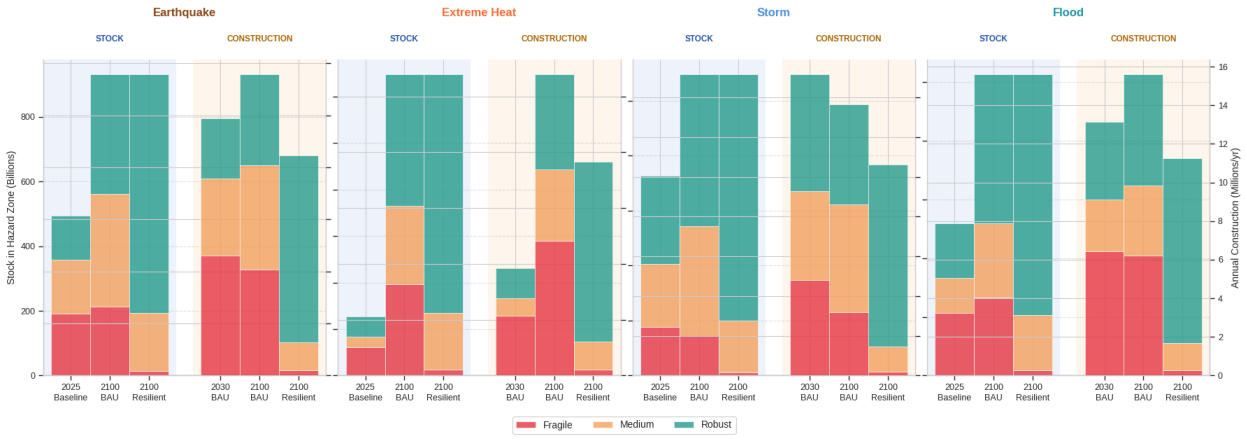


Note: Map projection: WGS 84 / UTM Zone 43N (EPSG:32643). Spatial resolution: 1 km. The flood hazard layer is sourced from the World Resources Institute Aqueduct Flood Hazard Maps, Version 2. Light blue areas indicate locations with projected flood depth exceeding 0.15 m in 2050 under the RCP 8.5 climate scenario.

The Resilient pathway generates two compounding benefits for housing in hazard-exposed areas, both visible in Figure 9. The first is a reduction in total annual construction volume within hazard zones. Because higher-quality housing survives longer, replacement demand falls over time, reducing the volume of new construction that must be absorbed by already-stressed institutional and fiscal systems. By 2100, annual construction in hazard-exposed areas is approximately 25 to 30 percent lower under the Resilient pathway than under BAU across all four hazard categories. The second and more immediate benefit is a transformation in the quality composition of that construction. Under BAU, fragile units continue to constitute a substantial share of new construction in hazard zones throughout the century. Approximately 6 million to 7 million units per year are constructed in flood- and earthquake-exposed areas by 2100. Under the Resilient pathway, fragile construction in hazard zones is effectively eliminated by mid-century, with nearly all new units built to robust standards by 2100.

These two effects combine to produce large reductions in the fragile stock located within hazard zones. Under SSP3, the number of fragile housing units in flood-exposed areas declines from approximately 133 million under BAU by 2050 to 58 million under Resilient (a reduction of 57 percent), and falls further to 9 million by 2100 under Resilient compared to 133 million under BAU. The same pattern holds across all hazard categories: fragile units in earthquake-, heat-, and storm-exposed areas are reduced by 55 to 60 percent by 2050 and by 90 to 95 percent by 2100 under the Resilient pathway relative to BAU. This resilience dividend is robust across all SSP scenarios, with the magnitude of the fragile stock reduction remaining consistent.

Figure 9 Housing Stock and New Construction in Hazard Zones: Comparison between BAU and Resilient Pathways (SSP3)



Affordability of the Resilient Pathway

Across all SSP scenarios, global annual housing construction costs expressed in absolute terms increase substantially over the projection period, before moderating toward the end

of the century (Figure 10). The absolute cost levels differ considerably by scenario. SSP5 generates the highest cumulative demand, with BAU construction costs approaching approximately $20 trillion annually by 2100, while SSP3 remains comparatively lower, stabilizing at around $10 trillion per year. This major difference is due to the fact that SSP5 has the highest GDP per capita trajectory of all five SSPs. It is important to note that this cost does not include land, infrastructure, and other requirements for new housing developments.

The Resilient Policy pathway involves higher absolute costs than BAU in the near to medium term, with a reversal emerging in the latter decades of the century in most regions. This initial spending premium reflects the greater unit cost of median- and robust-standard construction relative to fragile housing. However, as a more durable stock progressively reduces the volume of replacement construction required, annual spending under the Resilient pathway eventually falls below BAU. This crossover point, which marks the beginning of what the paper refers to as the payoff zone, occurs between approximately 2060 and 2070 depending on the scenario.

Figure 10 *Global Annual Housing Construction Cost (Billion USD PPP): BAU vs Resilient Policy*

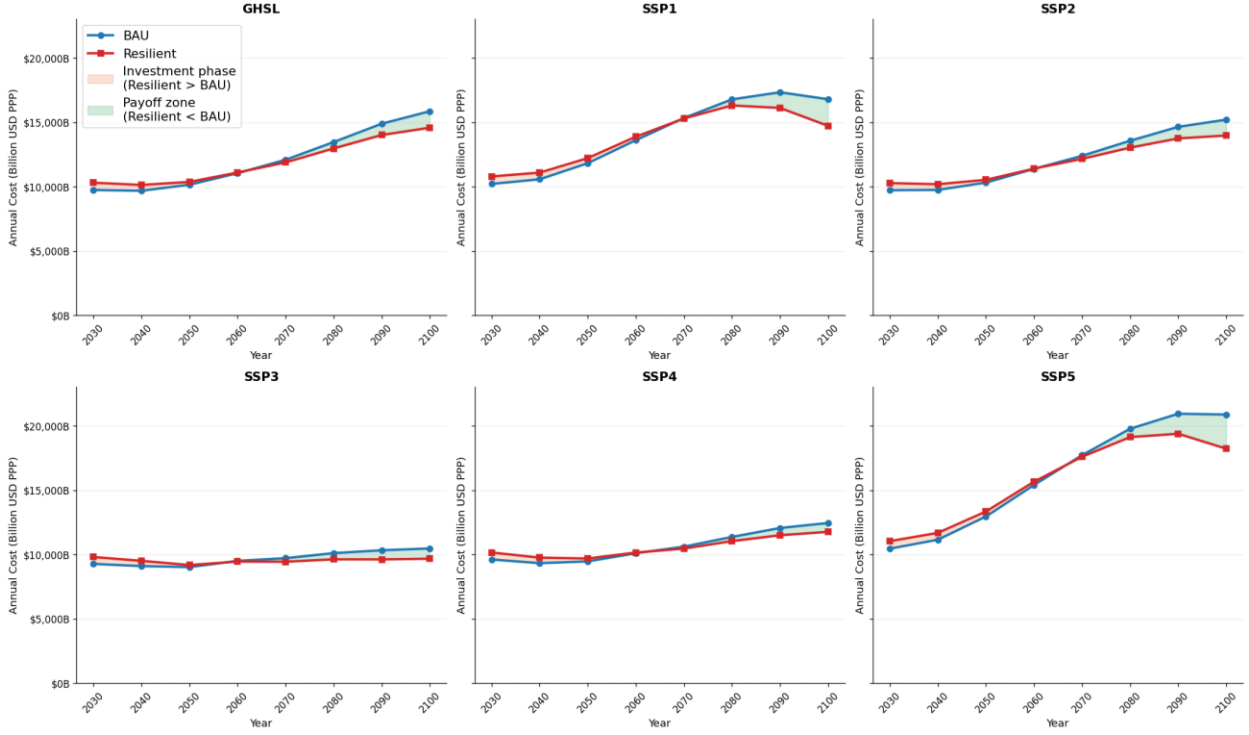
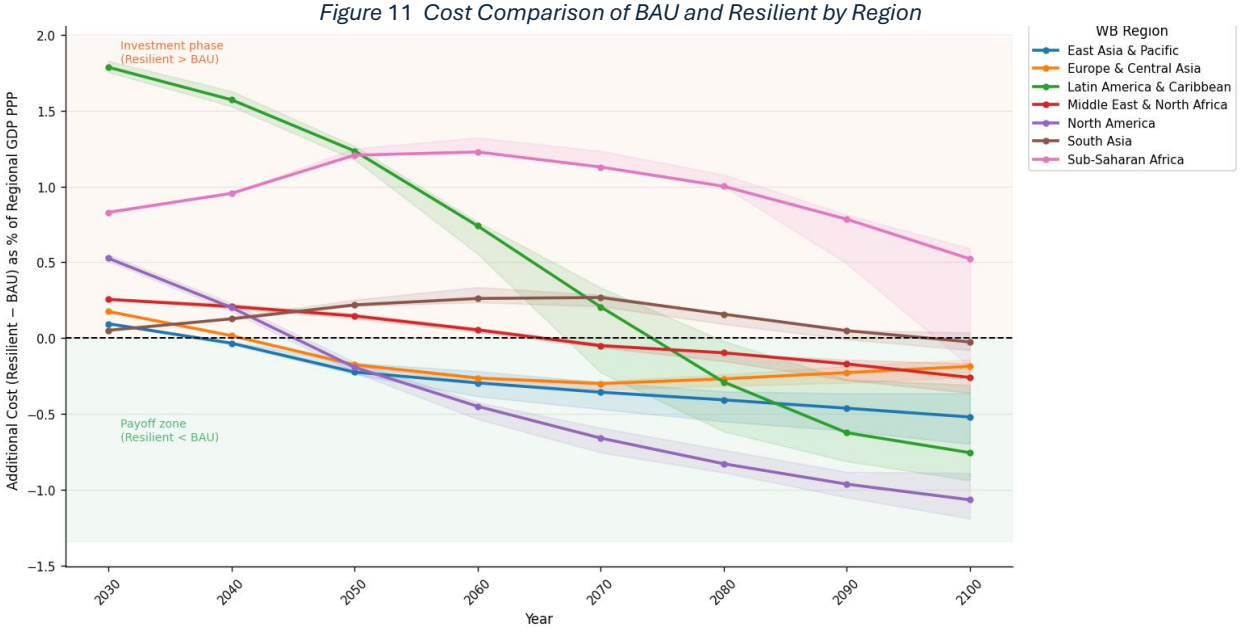


Figure 11 disaggregates this expenditure comparison by World Bank region and expresses it as a share of projected GDP, revealing important differences in both the magnitude and timing of cost dynamics. In East Asia and the Pacific, Europe and Central Asia, and North America, annual construction expenditure under the Resilient scenario falls below BAU

relatively early, generally between 2040 and 2050 depending on the SSP scenario. These regions benefit from stabilizing or declining construction volumes as demographic pressures ease, which allows the durability premium of higher-quality stock to reduce replacement needs within a shorter time horizon. In the Middle East and North Africa and in Latin America and the Caribbean, the crossover occurs later, generally between 2060 and 2080 across most scenarios.

The picture is markedly different for South Asia and Sub-Saharan Africa. In these regions, sustained high construction volumes mean that upgrading half of new construction to a higher quality standard generates a persistent spending premium throughout the projection period. The Resilient scenario remains more costly than BAU on an annual basis across virtually all scenarios, with only a marginal convergence for some SSP trajectories in South Asia near 2100. Since this analysis measures construction expenditure and does not account for avoided disaster losses, the full economic case for resilient investment in these regions cannot be assessed from cost data alone. Quantifying those benefits remains an important direction for future work.

Figure 11 Cost Comparison of BAU and Resilient by Region



Note: Line shows the SSP 2. Sharded band shows the range of all SSP scenarios.

Small Island Developing States (SIDS) represent a further category of concern. These countries face a disproportionate expenditure burden under the Resilient scenario due to the combination of acute hazard exposure, limited construction scale economies, and high unit costs. In the 2040–2050 period, construction costs as a share of projected GDP PPP under the Resilient scenario exceed BAU by over 30 percentage points in Solomon Islands

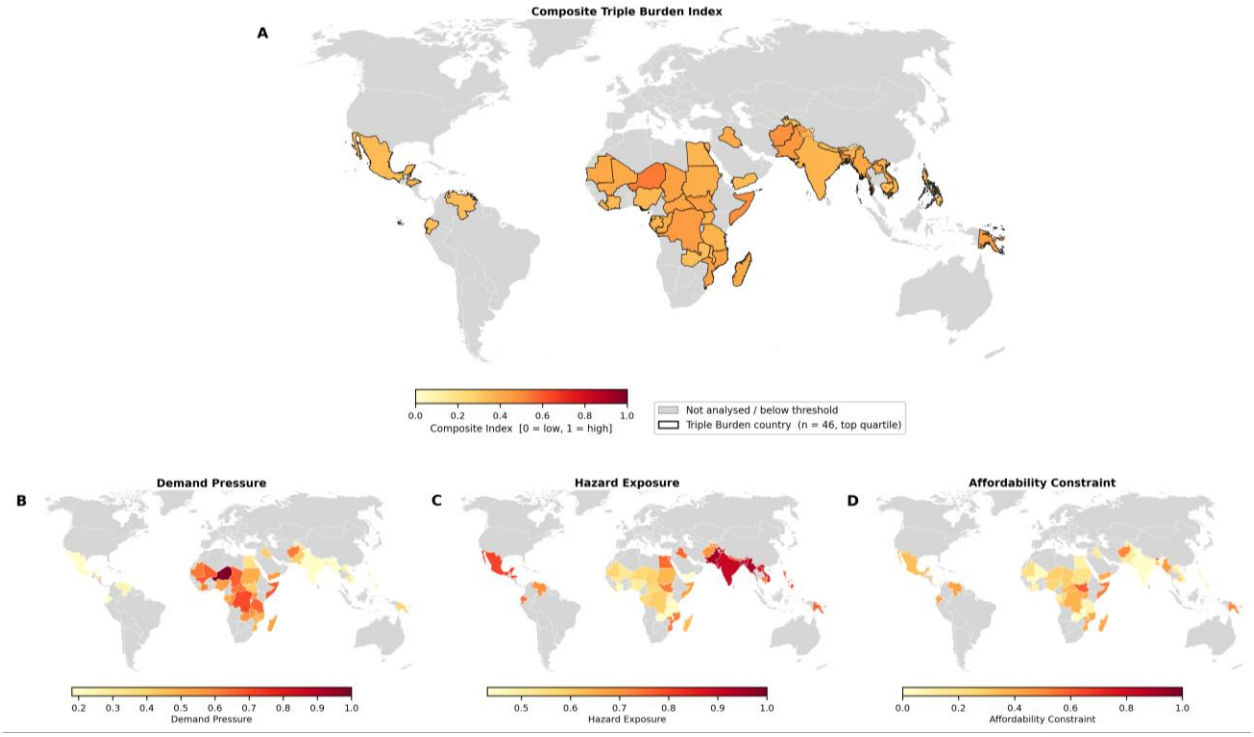
and Vanuatu — levels that are unlikely to be fiscally sustainable without dedicated international support.

Triple Burden Classification

The composite index identifies 46 triple burden countries, defined as those in the top quartile (threshold: 0.334; Figure 12, Figure A3-1, A3-2, A3-3). Sub-Saharan Africa dominates the group with 21 countries, driven primarily by extreme demand pressure: Niger records the highest demand pressure score in the full sample. Pacific small island states, where Vanuatu, Solomon Islands, and Tonga, ranked first, second, and twenty-third overall, are distinguished instead by fiscal incapacity. In South and Southeast Asia, hazard exposure is the primary driver: Bangladesh records the highest multi-hazard exposure score in the full sample, and India enters the group at rank 28 despite low fiscal incapacity and modest demand pressure. In Latin America and the Caribbean, five countries qualify through moderate scores across all three dimensions simultaneously rather than through extreme performance on any single one. One country from Europe and Central Asia and three from the Middle East and North Africa also appear, reflecting combinations of hazard exposure and demand pressure that exceed the threshold despite limited fiscal stress. Of the 46 countries, 37 are low or lower-middle income. Scenario range bars confirm that triple burden classification is robust across all six SSP scenarios for most identified countries, indicating that the structural disadvantages driving these results are not contingent on any single population trajectory.

The three burden dimensions are largely independent across the full sample of 181 countries (Annex 3). Demand pressure and hazard exposure show near-zero and statistically non-significant correlation, confirming that high construction volume and high hazard exposure are distinct phenomena requiring separate assessment. Hazard exposure and affordability constraint show a modest but significant association. The strongest association is between demand pressure and affordability constraint, reflecting the tendency for high-growth countries to also face greater fiscal pressure from resilient construction Despite this association, the composite identifies countries where all three burdens converge beyond what any single indicator would reveal.

Figure 12 Triple Burden Index Across All Analyzed Countries (2025-2100)



Note: Panel A: Composite Triple Burden Index across all analyzed countries. Black outlines mark top-quartile (Triple Burden) countries. Panels B–D: Individual burden scores for Triple Burden countries only, rescaled to each indicator's observed range. Affordability Constraint is log-scaled for display. Worst-case values across demographic scenarios (GHSL, SSP1–SSP5).

Sensitivity Analysis Results

Results are robust across the range of parameter assumptions tested, but the magnitude of sensitivity varies substantially across dimensions.

Building lifespan. Replacement requirements are most sensitive to the short lifespan scenario. Halving the fragile lifespan from 20 to 10 years increases cumulative replacement demand by approximately 63 percent by 2050 and 33 percent by 2100 relative to the central baseline. The larger relative effect in the earlier period reflects the rapid cycling of the large inherited 2025 fragile stock, through replacement at twice the baseline rate. Under the long lifespan scenario, extending fragile lifespans to 25 years reduces cumulative replacement volumes by approximately 20 percent across both time horizons relative to the baseline.

Table 2 Sensitivity Check: Implications of Shorter and Longer Lifespan

Lifespan	Year	Cumulative replacement (M units)	Δ Replacement (M)
Central (baseline)	Cumulative to 2050	2,184.3	-
	Cumulative to 2100	7,765.8	-
Short lifespan	Cumulative to 2050	3,550.3	1,366.0
	Cumulative to 2100	10,327.0	2,561.2
Long lifespan	Cumulative to 2050	1,742.3	(442.0)
	Cumulative to 2100	6,302.8	(1,463.0)

Governance implementation capacity. The governance sensitivity analysis isolates the role of regulatory enforcement in determining how rapidly the Resilient pathway improves housing quality. Under low implementation (25 percent upgrading), the fragile housing share under the Resilient pathway reaches 24.7 percent by 2050, roughly 8.8 percentage points above the moderate-governance baseline of 15.9 percent. Under high implementation (75 percent upgrading), the fragile share falls to 9.9 percent by 2050, approximately 6 percentage points below baseline. By 2100, differences narrow considerably as cumulative stock turnover reduces the influence of any single decade's construction standards: the range across governance scenarios spans 0.9 to 6.0 percent fragile, compared to 1.8 percent under the baseline.

Table 3 Sensitivity Check: Governance Implementation Capacity for Resilient Pathway

Governance assumption	Year	Fragile share (%)	Robust share (%)
Low governance (25% upgrade)	2050	24.7	43.7
	2100	6.0	64.0
Moderate governance baseline (50% upgrade)	2050	15.9	51.1
	2100	1.8	79.3
High governance (75% upgrade)	2050	9.9	58.8
	2100	0.9	88.0

Natural hazard thresholds. The results demonstrate that reported at-risk shares are highly sensitive to the choice of hazard severity threshold. Under the stricter second-threshold variant, measured hazard exposure falls sharply relative to the baseline. Heat exposure is the most threshold-sensitive metric, declining by 36.6 percentage points by 2050 and by 21.1 percentage points by 2100 relative to the main thresholds. This implies that a substantial portion of housing classified as heat-exposed under the baseline thresholds is situated in zones of moderate rather than severe thermal stress for 2050, but it will increase dramatically in consideration of future temperature increase toward 2100.

Table 4 Sensitivity Check: Housing Stock Exposure to Natural hazards (baseline and stricter thresholds - %)

variant	year	Earthquake	Heat	Storm	Flood
Main threshold (baseline)	2050	20.6	41.4	16.1	10.9
	2100	20.5	71.4	12.1	11.3
Second (stricter) threshold	2050	5.2	4.8	5.9	5.4
	2100	5.0	50.3	4.4	6.3

Model Validation

The hierarchical validation covers 3,007 back-casting observations at the 2005 cutoff, comprising 2,839 subnational unit observations across 87 countries and 168 national observations across 50 countries. The model achieves an overall Mean Absolute Percentage Error (MAPE) of 6.3 percent, a Root Mean Square Error (RMSE) of 0.408 persons, and a Mean Absolute Error (MAE) of 0.259 persons. Results at the 2008 cutoff are consistent, confirming robustness to the choice of validation period (Table 5).

Table 5 Back-casting validation results.

Cutoff	Level	Observations	MAPE	RMSE	MAE	RMSE (no offset)	MAE (no offset)
2005 (Primary)	Overall	3,007	6.3%	0.408	0.259	0.753	0.476
2005 (Primary)	Subnational	2,839	6.3%	0.406	0.257	0.760	0.477
2005 (Primary)	National	168	7.2%	0.444	0.285	0.630	0.467
2008 (Secondary)	Overall	2,415	6.1%	0.366	0.239	0.770	0.475
2008 (Secondary)	Subnational	2,289	6.0%	0.363	0.236	0.768	0.471
2008 (Secondary)	National	126	7.2%	0.420	0.300	0.806	0.549

The offset layer reduces MAE by approximately 46 percent relative to the raw model prediction at both cutoffs, confirming that country- and subnational-level calibration captures systematic variation that the global regression does not fully explain. Subnational predictions are marginally more accurate than national predictions, consistent with the expectation that subnational offsets anchor projections to more granular local conditions. Validation figures are provided in Annex 4.

5. Discussion

This study projected that the global housing stock will nearly double by the year 2100, reaching between 4.1 billion and 4.5 billion units, depending on the scenario. Notably, population size alone cannot predict aggregate housing requirements across scenarios. Although the population under SSP3 is 4.9 billion larger than under SSP5 by 2100, the required housing stock is similar in both scenarios. This reflects how rising incomes under SSP5 lead to smaller households, effectively offsetting the lower population count. The implication for policy makers is that strategies for housing investment calibrated to

population projections alone risk systematic error, particularly in economies with high income growth.

The construction quality decisions made in the coming decades will determine the burden of replacing housing for the rest of the century. Throughout this study, the Resilient pathway refers to a scenario in which new construction progressively shifts away from fragile building typologies toward median- and robust-quality standards. Fragile buildings have shorter service lives and require earlier replacement, which compounds fiscal pressure when new construction demand remains high. The resilient construction pathway reduces annual replacement requirements by 34 to 40 percent compared to business as usual by the 2090s. In most regions, construction expenditure under the resilient pathway converges with and then falls below the BAU trajectory between 2060 and 2070. This expenditure crossover, however, should be read alongside the scope of the analysis: the model captures construction expenditure only and does not quantify avoided disaster losses, reduced maintenance burdens, or the welfare costs of continued fragile housing. The durability effect alone drives the crossover observed in low-to-moderate growth regions. In high-growth, high-hazard regions such as South Asia and Sub-Saharan Africa, where sustained construction volumes prevent the crossover from materializing within the century, the full economic return to resilient investment is more likely to be realized through avoided losses than through lower construction volumes. Assessing that return would require a separate benefit estimation and remains an important direction for future work.

The heterogeneity among the 46 triple burden countries has direct implications for national policy as well as international support. In countries where fiscal incapacity is the main constraint, such as Pacific small island states, national governments have comparatively limited room to act alone, and concessional financing and dedicated climate finance mechanisms are the priority, since reducing the upfront cost premium of resilient construction is what determines whether the long-term savings from lower replacement costs are ever realized. In regions where demand pressure dominates, such as much of Sub-Saharan Africa, the most urgent need is to establish and enforce building standards before the majority of construction occurs, since regulatory action taken now applies to construction that has not yet occurred. In regions where hazard exposure is the primary driver, such as South and Southeast Asia, spatial planning and land use policy are as important as construction quality, because a well-built house in a highly exposed location still carries substantial residual risk. It is worth clarifying that this study measures hazard exposure, meaning the physical presence of housing stock in zones of hazard occurrence, rather than disaster risk in the fuller sense, which also depends on the vulnerability of specific structures and populations and the value of what stands to be lost.

Several limitations should be noted. First, hazard projections were not fully aligned with population projection scenarios across all reference years, requiring temporal interpolation and scenario-matching assumptions that introduce uncertainty. Flood hazard mapping at 1 km resolution is also likely insufficient to capture local exposure differences in topographically complex or densely urbanized areas. Second, the analysis captures housing requirements driven by demographics rather than effective demand based on purchasing power, and the projections therefore represent an upper-bound estimate of need rather than a forecast of actual construction. The affordability assessment operates at the country level and does not reflect the distribution of constraints across individual households. Third, the building lifespan assumptions are held uniform across all contexts; in practice, effective service lives vary with the speed and form of urbanization and differ between urban and rural settings.

Beyond these data and measurement constraints, several modeling choices also bear on how the results should be interpreted. The resilient scenario assumes full replacement of fragile stock rather than partial retrofitting or incremental rehabilitation, which is the more common pathway in informal settlements; the cost and effectiveness profiles of progressive improvement programs are not captured in the current framework. The model also does not account for disaster shocks or climate-driven migration, both of which can alter the spatial distribution and timing of housing demand in ways that smooth depreciation functions cannot represent. The three burden dimensions are, in addition, treated as independent in the composite index, but climate change is likely to drive both hazard exposure and, through recurrent disaster losses, the erosion of fiscal capacity in exposed countries, an interaction this study does not capture and one that implies the fiscal burden facing high hazard-exposure countries may be understated rather than overstated. Finally, the equal weighting of the triple burden index components is a normative choice; in most policy applications, the individual burden scores are more directly actionable than the composite, and alternative weighting schemes could alter country classifications at the margin.

6. Conclusion

This study is the first to provide a spatially explicit, multi-hazard, multi-scenario assessment that links housing demand, disaster risk exposure, and fiscal capacity across 181 countries through the year 2100. The results show that long-term resilient construction expenditure falls below business as usual in most regions, driven by the durability effect of higher-quality stock reducing replacement volumes over time. The transition from population growth–driven to replacement-driven construction will redefine the housing challenge in most regions by mid-century. Finally, the triple burden classification offers

international development partners a quantitative, regionally differentiated basis for prioritizing support, with Pacific small island states facing acute fiscal constraints, Sub-Saharan Africa facing an unprecedented volumetric demand challenge, and South and Southeast Asian countries facing the highest hazard exposure as the primary risk driver.

The global framework developed here is designed as a foundation for more granular applications. Translating the methodology to the country and city levels using local building stock inventories, local hazard assessments, and specific demographic and fiscal parameters would substantially improve the framework's accuracy. This would allow the results to be used directly for housing sector strategies, urban planning decisions, and disaster risk management policies in an integrated way. At that scale, the analysis can inform how much housing is needed, where it should be located, what standards are appropriate, what fiscal pathways are realistic, and how land use and risk reduction investments should be sequenced. The author considers this localization to be the most important direction for future work. Ultimately, most of the housing that will stand in 2100 has not yet been built, and the decisions on standards and location made over the next decades will shape disaster risk, fiscal exposure, and the quality of life for billions of people for the remainder of the century.

7. Acknowledgments

This study was conducted as part of the Global Program for Resilient Housing at the Global Facility for Disaster Reduction and Recovery (GFDRR), World Bank. The author is grateful to Niels B. Holm-Nielsen, Ana Campos, and Keiko Saito for their guidance throughout this work. Technical inputs and review were provided by Luis Triveno, Sarah Antos, and Jessica Goldsmith (Global Program for Resilient Housing) and Aaron Opdyke and Keiko Sakoda (Building Regulation for Resilience). The paper benefited from peer review by Carlos Ariel Cortes, Jun Rentschler, and Ross Marc Eisenberg. The author also appreciates helpful exchanges with Catherine Lynch and Su Jung Song of the Global Housing team. Eigo Tateishi provided support on GIS and GEM subnational mapping. Advice on heat analysis was generously shared by Nicholas K.W. Jones and Daniel Zepeda Rivas.

The research was made possible with the financial support from the Japan–World Bank Program for Mainstreaming Disaster Risk Management in Developing Countries, which is finance by the Government of Japan and receives technical support from the World Bank GFDRR Tokyo Disaster Risk Management Hub.

The findings and interpretations expressed in this paper are those of the author and do not necessarily reflect the views of the World Bank, its Executive Directors, or the governments they represent

8. References

Aktas, C. B., & Bilec, M. M. (2012). Impact of lifetime on US residential building LCA results. *The International Journal of Life Cycle Assessment*, *17*(3), 337–349. https://doi.org/10.1007/s11367-011-0363-x

Bathurst, M. (2023). *Architectural Longevity: What Determines a Building's Lifespan?* MIT Architecture

Behr, D. M., Chen, L., Goel, A., Haider, K. T., Singh, S., & Zaman, A. (2021). Introducing the Adequate Housing Index: A New Approach to Estimate the Adequate Housing Deficit within and across Emerging Economies. *Policy Research Working Paper;No. 9830*. https://doi.org/10.1596/1813-9450-9830

Bloemendaal, N., de Moel, H., Dullaart, J., Haarsma, R. J. R., & Haigh, I. D. I. (2023). *STORM climate change tropical cyclone wind speed return periods. Version 4. 4TU.ResearchData. dataset.* (https://doi.org/10.4121/14510817.v4

Bloemendaal, N., de Moel, H. H., Muis, S., Haigh, I. D. I., & Aerts, J. C. J. H. J. (2023). *STORM tropical cyclone wind speed return periods. Version 4. 4TU.ResearchData. dataset.* (https://doi.org/10.4121/12705164.v4

Bondarenko, M., Tejedor-Garavito, N., Priyatikanto, R., Zhang, W., Fang, W., Nosatiuk, B., Gaskell, J., McKeen, T., Noi, E., Hilton, J., Butterick, J., Hawker, L., & Tatem, A. J. (2025). *Global 1km-grid population projections for 2025-2100 consistent with the Shared Socioeconomic Pathways 3.2 national population projections, version 0.2* (https://doi.org/10.5258/SOTON/WP00849

Chen, S., Huang, Q., Muttarak, R., Fang, J., Liu, T., He, C., Liu, Z., & Zhu, L. (2022). Updating global urbanization projections under the Shared Socioeconomic Pathways. *Scientific Data*, *9*(1), 137. https://doi.org/10.1038/s41597-022-01209-5

Dijkstra, L., Florczyk, A. J., Freire, S., Kemper, T., Melchiorri, M., Pesaresi, M., & Schiavina, M. (2021). Applying the Degree of Urbanisation to the globe: A new harmonised definition reveals a different picture of global urbanisation. *Journal of Urban Economics*, *125*, 103312. https://doi.org/https://doi.org/10.1016/j.jue.2020.103312

Dodman, D. M., Hayward, B., Pelling, M., Broto, V., Chow, W., Chu, E., Dawson, R., Khirfan, L., McPhearson, T., Prakash, A., Zheng, Y., Ziervogel, G., Archer, D., Bertolin, C., Brail, S., Cartwright, A., Chester, M., Colenbrander, S., Dhar, T., & Westman, L. (2022). Cities, Settlements and Key Infrastructure.

Esteve, A., Pohl, M., Becca, F., Fang, H., Galeano, J., García-Román, J., Reher, D., Trias-Prats, R., & Turu, A. (2024). A global perspective on household size and composition, 1970–2020. *Genus*, *80*(1), 2.

Galeano, J., Esteve, A., Turu, A., García-Roman, J., Becca, F., Fang, H., Pohl, M., & Trias-Prats, R. (2024). CORESIDENCE: National and subnational data on household size and composition around the world, 1964–2021. *Scientific Data*, *11*(1), 145. https://doi.org/10.1038/s41597-024-02964-3

Güneralp, B., Lwasa, S., Masundire, H., Parnell, S., & Seto, K. (2017). Urbanization in Africa: Challenges and opportunities for conservation. *Environmental Research Letters*, *13*. https://doi.org/10.1088/1748-9326/aa94fe

Hallegatte, S., Vogt-Schilb, A. C., Bangalore, M., & Rozenberg, J. (2016). *Unbreakable: Building the Resilience of the Poor in the Face of Natural Disasters*. https://doi.org/10.1596/978-1-4648-1003-9

Johnson, K., Villani, M., Bayliss, K., Brooks, C., Chandrasekhar, S., Chartier, T., Chen, Y., Garcia-Pelaez, J., Gee, R., Styron, R., Rood, A., Simionato, M., & Pagani, M. (2023). *Global Earthquake Model (GEM) Seismic Hazard Map (version 2023.1 - June 2023)* (https://doi.org/10.5281/zenodo.8409647

Knight Frank, & NAREDCO. (2025). *India Affordable Housing: Tackling Urban Housing Deficit Through Supply-Side Reforms*.

Kose, M. A., Kurlat, S., Ohnsorge, F., & Sugawara, N. (2022). A cross-country database of fiscal space. *Journal of International Money and Finance*, *128*, 102682. https://doi.org/https://doi.org/10.1016/j.jimonfin.2022.102682

Middelanis, R., Jafino, B. A., Hill, R., Nguyen, M. C., & Hallegatte, S. (2025). *Global Socio-economic Resilience to Natural Disasters*. https://doi.org/10.1596/1813-9450-11129

Rentschler, J., Avner, P., Marconcini, M., Su, R., Strano, E., Vousdoukas, M., & Hallegatte, S. (2023). Global evidence of rapid urban growth in flood zones since 1985. *Nature*, *622*(7981), 87–92. https://doi.org/10.1038/s41586-023-06468-9

Rentschler, J., Salhab, M., & Jafino, B. A. (2022). Flood exposure and poverty in 188 countries. *Nat Commun*, *13*(1), 3527. https://doi.org/10.1038/s41467-022-30727-4

Riahi, K., van Vuuren, D. P., Kriegler, E., Edmonds, J., O'Neill, B. C., Fujimori, S., Bauer, N., Calvin, K., Dellink, R., Fricko, O., Lutz, W., Popp, A., Cuaresma, J. C., Kc, S., Leimbach, M., Jiang, L., Kram, T., Rao, S., Emmerling, J.,...Tavoni, M. (2017). The Shared Socioeconomic Pathways and their energy, land use, and greenhouse gas emissions implications: An overview. *Global Environmental Change*, *42*, 153–168. https://doi.org/https://doi.org/10.1016/j.gloenvcha.2016.05.009

Sanjo, K., Kayo, C., & Tonosaki, M. (2025). Lifetime functions and half-lives of residential building structures in Japan: A comparative study of wooden, non-wooden, and concrete block houses. *Journal of Building Engineering*, *108*, 112916. https://doi.org/https://doi.org/10.1016/j.jobe.2025.112916

Schiavina, M., Melchiorri, M., Pesaresi, M., Jacobs-Crisioni, C., & Dijkstra, L. (2026). *GHS-WUP-DEGURBA R2025A – GHS-WUP DEGURBA settlement layers, application of the Degree of Urbanisation methodology (stage I) to GHS-WUP-POP R2025A, multitemporal (1975-2100)* (European Commission, Joint Research Centre. https://doi.org/10.2905/JRC.0Y84VH8

Shuker, I. G., Mahul, O., Bonte-Grapentin, M., Battaglini, E., Baca, A. C., Schuster, S., Dharmajaya, R. C., & Atamuratova, S. (2013). *Catastrophe risk assessment methodology : summary report (English)*. World Bank Group.

Stull, R. (2011). Wet-Bulb Temperature from Relative Humidity and Air Temperature. *Journal of Applied Meteorology and Climatology*, *50*(11), 2267–2269. https://doi.org/10.1175/jamc-d-11-0143.1

SwissLife. (2017). *What is the lifespan of a house?* https://www.swisslife.com/en/home/blog/what-is-the-lifespan-of-a-house.html

Tellman, B., Sullivan, J. A., Kuhn, C., Kettner, A. J., Doyle, C. S., Brakenridge, G. R., Erickson, T. A., & Slayback, D. A. (2021). Satellite imaging reveals increased proportion of population exposed to floods. *Nature*, *596*(7870), 80–86. https://doi.org/10.1038/s41586-021-03695-w

UN-Habitat. (2005). *Financing Urban Shelter: Global Report on Human Settlements 2005*.

UN-Habitat. (2025). *Annual Report 2024*. UN-Habitat.

United Nations Department of Economic and Social Affairs. (2019). Patterns and trends in household size and composition: evidence from a United Nations dataset. In: United Nations New York, NY, USA.

United Nations Department of Economic and Social Affairs. (2022). *Database on Household Size and Composition 2022* (

United Nations Department of Economic and Social Affairs. (2024). *World Population Prospects 2024: Summary of Results*. Stylus Publishing, LLC.

United Nations Office for Disaster Risk Reduction. (2025). *Global Assessment Report on Disaster Risk Reduction 2025: Resilience Pays: Financing and Investing for Our Future*. Stylus Publishing, LLC.

Wang, J., Zhang, Y., & Wang, Y. (2018). Environmental impacts of short building lifespans in China considering time value. *Journal of Cleaner Production*, *203*, 696–707. https://doi.org/https://doi.org/10.1016/j.jclepro.2018.08.314

World Bank. (2016). *From Oil to Cities: Nigeria's Next Transformation*. World Bank Publications.

World Bank. (2020). *Indonesia Public Expenditure Review 2020Kajian Belanja Publik Indonesia : Belanja untuk Hasil yang Lebih Baik*. https://doi.org/10.1596/33954

World Bank. (2021). *Striking a Balance: Toward a Comprehensive Housing Policy for a Post-COVID Colombia*. World Bank. https://doi.org/10.1596/36500

World Bank. (2024). *Poverty and Equity Assessment for El Salvador 2024 : Improving Lives and Livelihoods - Background Note 3 : Housing Deprivation in El Salvador*. World Bank Group.

World Bank. (2025). *World Bank Official Boundaries version 5* (

World Bank, Inter-American Development Bank, & Global Facility for Disaster Reduction and Recovery. (2025). *A Global Assessment of Building Regulation for Resilience Building Codes: Current Status and Evolving Needs to Promote Resilient, Green and Inclusive Buildings*. World Bank and the Inter-American Development Bank. https://doi.org/10.1596/43310

World Resources Institute. (2020). *Aqueduct Floods Hazard Maps* (

Yepes-Estrada, C., Baiguera, M., Calderon, A., Caruso, M., Costa, C., Gonzalez, D., Nafeh, A. M. B., Rao, A., & Silva, V. (2026). *Global Exposure Model* (https://doi.org/doi.org/10.5281/zenodo.8117363

Yepes-Estrada, C., Calderon, A., Costa, C., Crowley, H., Dabbeek, J., Hoyos, M. C., Martins, L., Paul, N., Rao, A., & Silva, V. (2023). Global building exposure model for earthquake risk assessment. *Earthquake Spectra*, *39*(4), 2212–2235. https://doi.org/10.1177/87552930231194048

Annex

Annex 1: Expected Lifespans of Different Housing Quality Tiers

For the Fragile tier, the study sets L_q at 20 years. This estimate derives from averaging the lifespan of traditional housing in Pacific Island countries, typically 4–5 years for timber pole and bamboo frame structures, though some may last 20–30 years (Shuker et al., 2013), with the lower bound of residential building lifespans in China, estimated at 25–35 years(Wang et al., 2018).

The Median tier assumes a 40-year lifespan, corresponding to the lower bound of housing durability observed in the United States (50–63 years;(Aktas & Bilec, 2012; Bathurst, 2023)). This figure aligns closely with evidence from Japan, where non-wooden residential buildings exhibit half-lives of 50–59 years (Sanjo et al., 2025), compared to 29–75 years for wood construction depending on the construction period.

For the Robust tier, the study adopts a 60-year lifespan. This estimate reflects the upper range of building half-lives in Japan and is lower side of broader evidence from Europe, where many residential buildings remain in use for 70–100 years (SwissLife, 2017).

Annex 2: Household Size Projection Specification Robustness Tests

This annex presents four complementary tests to assess whether pooled OLS is an appropriate specification for long-run structural projection of average household size (AHS). The tests follow a logical sequence: a Hausman-style comparison of OLS and country fixed effects (Section A2.1); a Mundlak-Chamberlain correlated random effects test to decompose within-country and between-country effects (Section A2.2); a four-way coefficient comparison across OLS, fixed effects, between effects, and within-OLS specifications (Section A2.3); and a random slopes multilevel model to assess the degree of cross-country slope heterogeneity (Section A2.4).
The dataset covers 172 countries from 1990 to 2021 (N = 984). Countries with only a single observation were excluded from fixed effects estimation, as identification requires within-country temporal variation, reducing the FE sample to 966 observations.

A2.1 Hausman-Style Test: OLS versus Country Fixed Effects

A Hausman-style test was conducted to assess whether systematic differences exist between OLS and country fixed effects (FE) coefficient estimates. The Hausman test statistic is $H = 64.88$ ($df = 4$, $p < 0.001$), rejecting the null hypothesis that OLS and FE estimates are equivalent. This indicates that country-level unobserved heterogeneity is correlated with the regressors. This is as expected in a cross-country panel spanning diverse economic and demographic contexts. This result alone does not determine which specification is more appropriate for projection. FE identifies coefficients from within-country temporal variation, while OLS captures the cross-country structural gradient. For long-run projection to 2100, the cross-country gradient is the more relevant signal. Sections A2.2 and A2.3 examine this point in more detail and provide the empirical basis for retaining OLS as the main projection specification.

A2.2 Between-Effects and Within-Effects Decomposition

To assess whether OLS coefficients are driven by cross-country differences or within-country temporal change, a Mundlak-Chamberlain correlated random effects test was conducted by adding country-level means of each regressor to a random effects model. A likelihood ratio test confirms that these country means are jointly significant ($LR = 33.69$, $df = 4$, $p < 0.001$), with age structure variables (child rate and elderly rate) as the main source of divergence between OLS and FE estimates. Table A2.5 reports coefficients from four specifications side by side.

The OLS coefficients are consistently closer to the between-effects estimates than to the FE estimates, and the between-effects R^2 (0.796) is the highest across all specifications. This confirms that OLS is predominantly driven by cross-country structural differences,

which is the more relevant source of information for long-run projection. The only sign difference across specifications is for the urbanization rate, which is statistically insignificant in OLS and near zero in magnitude. This has no material consequence for projection outcomes.

Table A2.1. Coefficient Comparison Across Specifications

Variable	OLS	FE (Within)	Between
Log(GDP per capita)	-0.0594***	-0.0389***	-0.0408
	(0.022)	(0.014)	
Urban Rate	0.0005	-0.0021***	-0.0006
	(0.001)	(0.001)	
Child Rate (0-14)	0.0087***	0.0147***	0.0057
	(0.003)	(0.001)	
Elderly Rate (65+)	-0.0266***	-0.0092***	-0.0361
	(0.004)	(0.002)	
R^2	0.7913	0.5898	0.7961
N	984	966	172

*Standard errors in parentheses, clustered by country. * p < 0.10, ** p < 0.05, *** p < 0.01. Significance stars are reported for OLS and FE only, as the between-effects model is estimated on country means (N = 172 countries) rather than country-year observations, and standard inference is not directly comparable across specifications.*

A2.3 Random Slopes Multilevel Model

The previous sections confirm that OLS captures cross-country structural differences well, but a remaining question is whether the effect of GDP per capita on AHS is sufficiently consistent across countries to justify a single global coefficient. To test this, a random slopes multilevel model was estimated, allowing the GDP slope to vary across countries. The results are reported in Table A2.2.

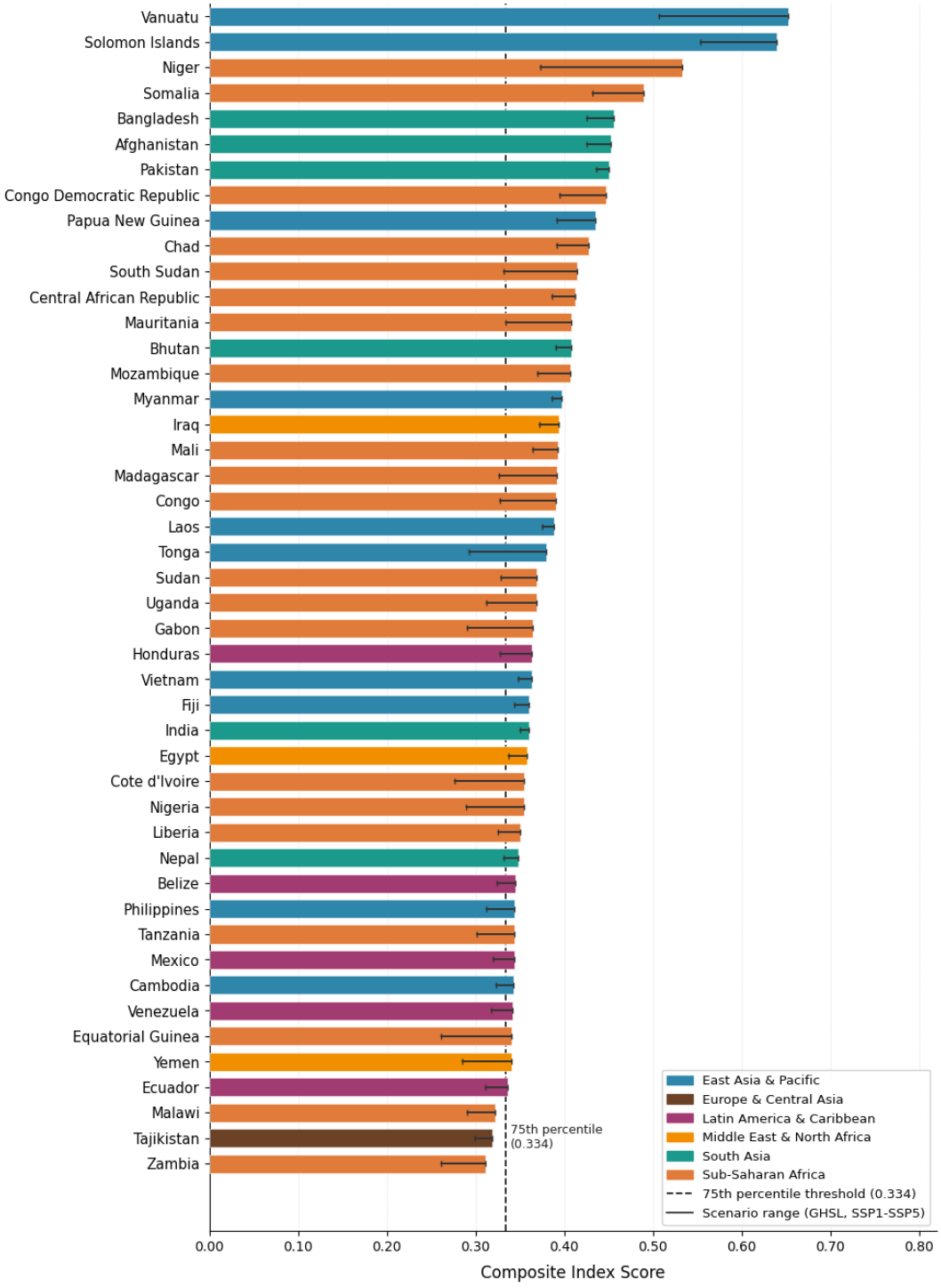
The slope varies across countries with a standard deviation of 0.011, which is about 36 percent of the global slope. This indicates some heterogeneity, but a likelihood ratio test finds no statistical evidence that the random slopes model fits better than the simpler random intercept model (p = 1.000). The global slope assumption is therefore supported.

Table A2.2. Random Slopes Model: GDP per Capita Slope

Statistic	Value
Global GDP slope (fixed effect)	-0.0296
Slope standard deviation across countries	0.0107
Slope variation relative to global slope	36%
Log-likelihood: random intercept model	1179.07
Log-likelihood: random slopes model	1176.54
LR test (df = 2)	p = 1.000

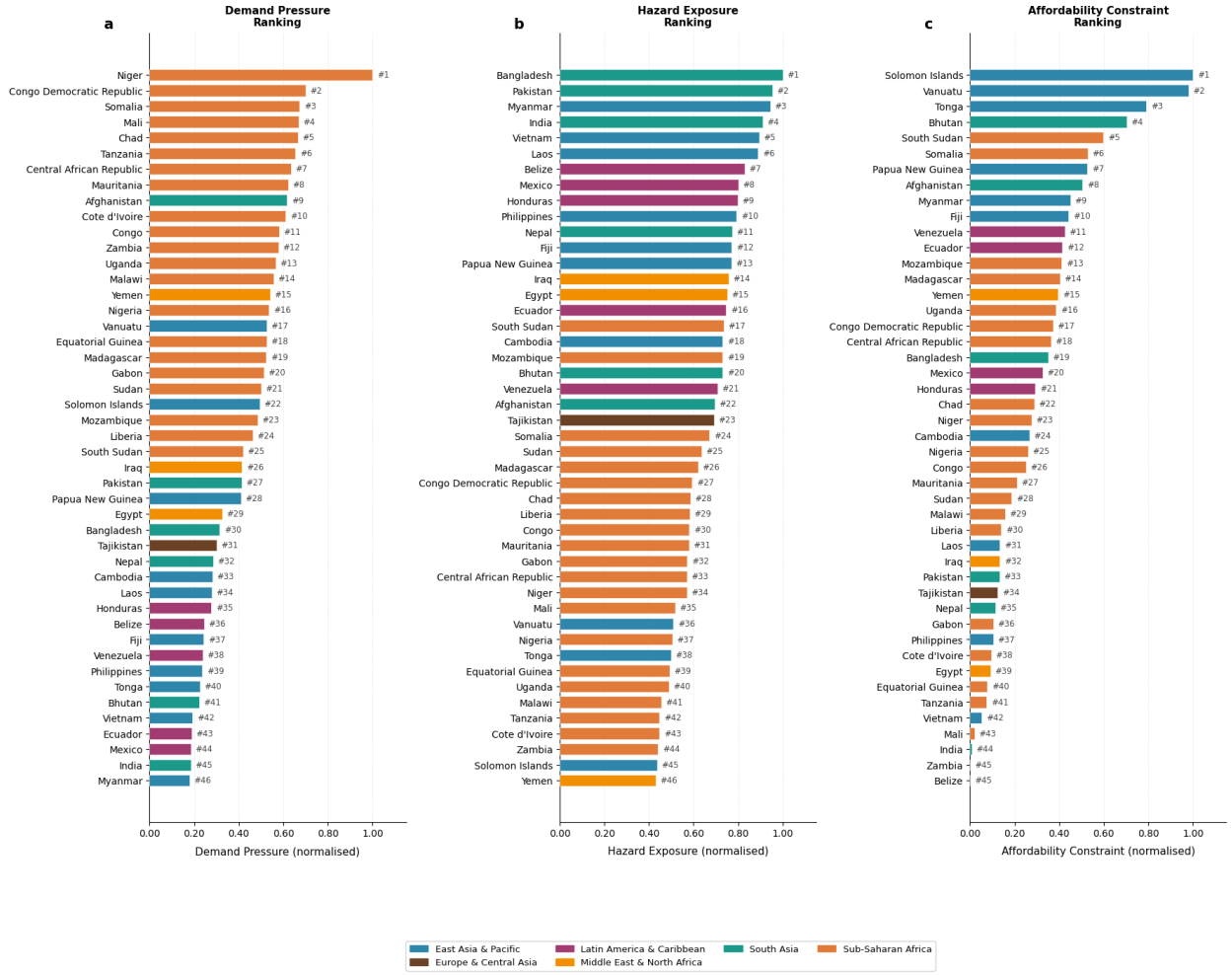
Annex 3: Triple Burden Index Decomposition

Figure A3-1: Triple Burden Countries: Composite Index



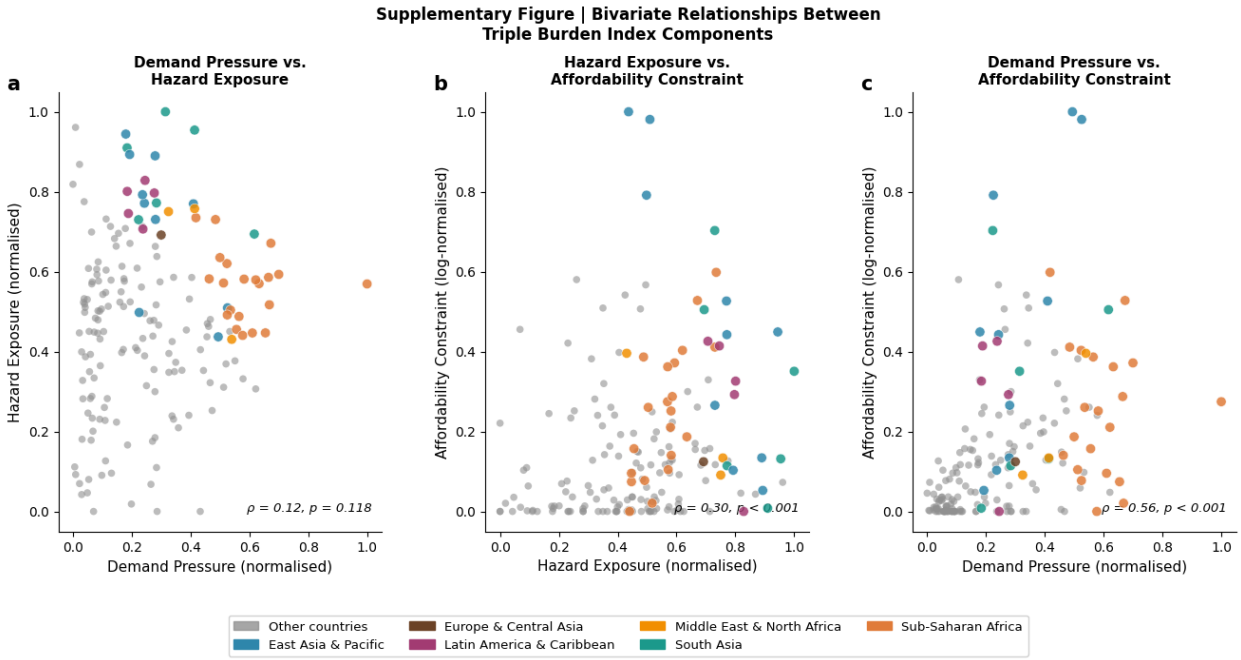
Note: All 46 triple burden countries (top quartile of composite index) ranked by composite score, color-coded with a breakdown by demand pressure, hazard exposure, and fiscal incapacity. Bars show the worst-case composite score across six demographic scenarios (GHSL, SSP1–SSP5)

Figure A3-2: Individual Burden Rankings



Note: Affordability Constraint is log-scaled for display.

Figure A3-3: Bivariate relationships between triple burden index components



Note: Bivariate relationships between the three normalised components of the Triple Burden Composite Index across all 181 countries. Triple burden countries (n = 46) are colour-coded by World Bank region; grey points represent other countries. Affordability Constraint axes use logarithmic scale; zero values are plotted at 1x10^-4 for log transformation and represent countries where resilient construction costs less than business-as-usual. Spearman rank correlation coefficients (ρ) and p-values are shown for each panel. The near-zero and non-significant correlation in panel a (ρ = 0.12, p = 0.118) confirms that demand pressure and hazard exposure are largely independent dimensions, validating the composite framing. A moderate correlation between hazard exposure and affordability constraint (panel b, ρ = 0.30, p < 0.001) and a stronger association between demand pressure and affordability constraint (panel c, ρ = 0.56, p < 0.001) suggest partial overlap, though the composite captures countries where all three burdens simultaneously exceed the 75th percentile threshold.

Annex 4: Validation Coverage and Figures

Validation Coverage by Cutoff Year

Table A4-1: National coverage

Cutoff	Train Records	Hold-out Records	Countries Usable
1995	89	895	68
2000	184	800	94
2003	338	646	134
2005	371	613	135
2008	505	479	143
2010	549	435	142

Table A4-2: Subnational coverage

Cutoff	Train Records	Hold-out Records	Units Usable	Countries
1995	2,013	5,307	806	68
2000	2,675	4,645	923	81
2003	3,665	3,655	932	86
2005	3,899	3,421	936	87
2008	4,693	2,627	999	95
2010	4,960	2,360	999	95

Validation Figures

Each row shows results for one data level (subnational, top; national, bottom). Left panels: predicted versus observed AHS with the hierarchical offset applied. Middle panels: predicted versus observed without the offset. Right panels: distribution of absolute percentage errors with the offset.

Figure A4-1: Back-casting validation results (Cutoff = year 2005: Primary)

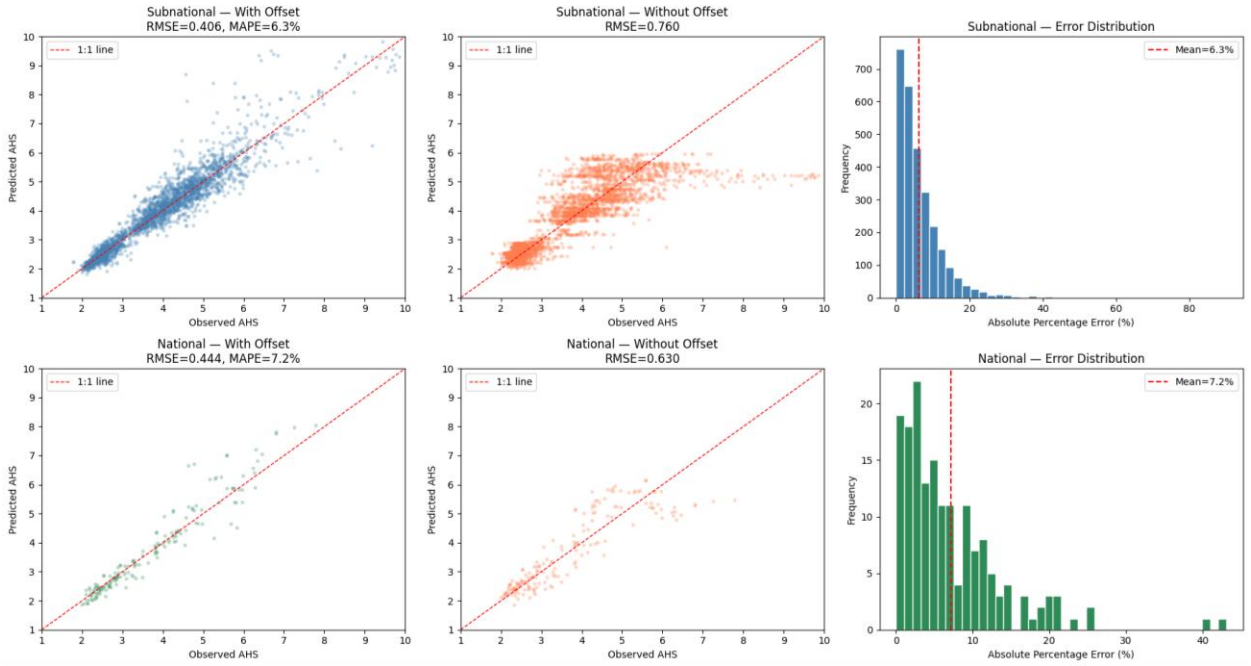
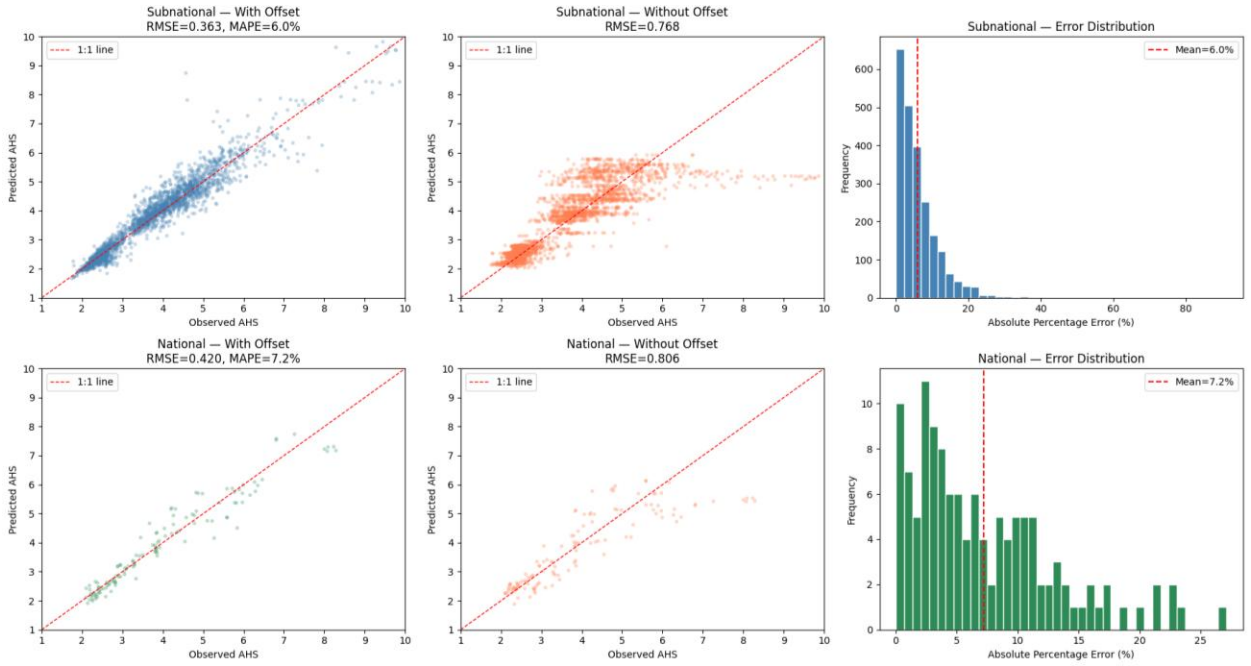


Figure A4-2: Back-casting validation results (Cutoff = year 2008: Secondary)



Annex 5: Additional Figures

Figure A5-1: Regional Housing Expansion: Existing Built-up vs Undeveloped Land (SSP3)

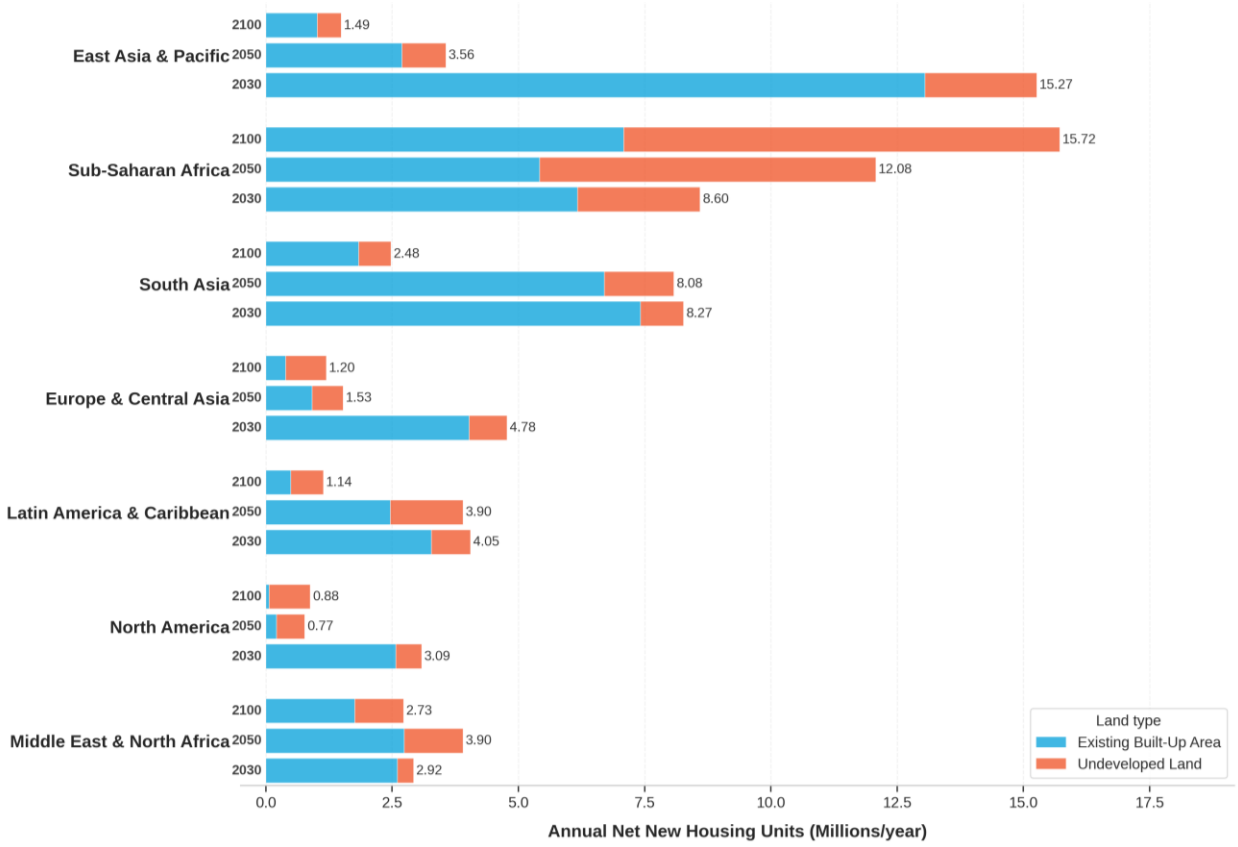


Figure A5-2: Global Projection of Housing Stock Exposure to Natural Hazards

